Exact results for a fully asymmetric exclusion process with sequential dynamics and open boundaries

Jordan Brankov,* Nina Pesheva, and Nikola Valkov
Institute of Mechanics, Bulgarian Academy of Sciences, Acad. G. Bonchev Str. 4, 1113 Sofia, Bulgaria
(Received 2 June 1999; revised manuscript received 13 October 1999)

An exact and rigorous calculation of the current and density profile in the steady state of the one-dimensional fully asymmetric simple-exclusion process with open boundaries and forward-ordered sequential dynamics is presented. The method is based on a matrix product representation of the steady-state probability distribution. The main idea is to choose a suitable representation in which the scalar products describing the current and local density profile for a chain of arbitrary finite size depend only on the elements in a finite number of rows and columns. This makes possible the use of a truncated finite-dimensional representation of the matrices and vectors involved. After performing the calculations, we lift the truncation by letting its dimensionality go to infinity. In this limit the results become exact for any size of the chain. By rescaling one of the infinite-dimensional matrix representations found in the work of Derrida *et al.* [J. Phys. A **26**, 1493 (1993)] for their algebra, we obtain a symmetric ''propagator'' matrix. Its truncated version is diagonalized by orthogonal transformation for easy calculation of the relevant scalar products. An interpretation of the phase transitions between the different phases is given in terms of eigenvalue splitting from a bounded quasicontinuous spectrum. A precise description of the local density profiles is given for all values of the parameters. It is shown that the leading-order asymptotic form of the position-dependent terms in the local density changes within the low- and high-density phases, signaling the presence of a higher-order transition.

PACS number(s): 05.60.−k, 02.50.Ey, 05.70.Ln, 64.60.Ht

I. INTRODUCTION

We consider the current and density profile in the steady state of a one-dimensional fully asymmetric simple-exclusion process (FASEP) on a chain of L sites, with open boundaries and forward-ordered sequential dynamics. Each site can be empty or occupied by exactly one particle. At each time step a particle is injected with probability α at the left end ($i=1$). Then each pair of nearest-neighbor sites is updated sequentially from the left to the right. A particle hops with probability p one site to the right, provided that site is empty. Finally, a particle is removed with probability β at the right end ($i=L$). Note that the dynamics under consideration can transport a particle by many sites to the right during one update of the chain. Let $\tau_i \in \{0,1\}$, $i=1,2,\ldots,L$, be the random occupation variable of site i in a given time step: $\tau_i=1$ if the site is occupied by a particle, and $\tau_i=0$ if it is empty. Let $P_{\rightarrow}(\tau_1,\tau_2,\ldots,\tau_L)$ be the steady-state probability of finding the chain in configuration $\{\tau_1,\tau_2,\ldots,\tau_L\}$.

In the case of random-sequential dynamics, a matrix-product representation of the steady-state probability distribution has been found by Derrida, Evans, Hakim, and Pasquier (DEHP) [1]. Their representation involves two square matrices, D and E, infinite dimensional in the general case, which satisfy a quadratic algebra, called DEHP algebra. Krebs and Sandow [2] proved that the stationary state of any one-dimensional system with random-sequential dynamics involving nearest-neighbor hoppings and single-site boundary terms can always be written in a matrix-product representation. When each lattice site can be in either of m states, the general matrix-product representation is based on $2m$ matrices which obey a quadratic algebra. In contrast, the more special case of the DHEP algebra uses only m generators. Fock representations of the general quadratic algebra have been studied by Essler and Rittenberg [3], who have found explicit representations in terms of infinite-dimensional tridiagonal matrices.

We follow here all the steps, except the last one, of the mapping of the algebra for the ordered-sequential update onto the DEHP algebra, suggested by Rajewski, Schadschneider, and Schreckenberg [4]. Then, starting from one of the infinite-dimensional matrix representations for the solution of the DEHP algebra given in [1], namely, D_3 and E_3, we obtain the corresponding tridiagonal matrices $\tilde{D}_3$ and $\tilde{E}_3$ that solve the bulk algebra for the ordered-sequential update and satisfy the boundary conditions. The propagator matrix $\tilde{C}_3=\tilde{D}_3+\tilde{E}_3$ has a special property which makes possible its transformation to a symmetric form by a simple renormalization of the basis vectors.

To be more specific, let us consider an auxiliary infinite-dimensional vector space $\mathcal{S}$ and its dual space $\mathcal{S}^{\dagger}$. We are looking for two matrices, D and E, acting on the vectors of $\mathcal{S}$, and two vectors, $|V\rangle \in \mathcal{S}$ and $\langle W| \in \mathcal{S}^{\dagger}$, such that the steady-state probability $P_{\rightarrow}(\tau_1,\tau_2,\ldots,\tau_L)$ is given by the scalar product

$$P_{\rightarrow}(\tau_1,\tau_2,\ldots,\tau_L)=Z_L^{-1}\left\langle W\left|\prod_{i=1}^{L}\left[\tau_i D+(1-\tau_i)E\right]\right|V\right\rangle. \tag{1.1}$$

Here Z_L is a normalization constant. It is convenient to

*Electronic address: brankov@bas.bg

choose the following column vectors as a basis in the configuration space $\{0,1\}$ of the ith site

$$|\tau_i=0\rangle=\begin{pmatrix}1\\0\end{pmatrix},\quad |\tau_i=1\rangle=\begin{pmatrix}0\\1\end{pmatrix}, \tag{1.2}$$

and define a column vector A with the matrices E and D as components,

$$A=\begin{pmatrix}E\\D\end{pmatrix}=E|0\rangle+D|1\rangle. \tag{1.3}$$

By using the orthonormal basis of vectors $|\tau_1,\tau_2,\ldots,\tau_L\rangle=|\tau_1\rangle\otimes|\tau_2\rangle\otimes\cdots|\otimes|\tau_L\rangle$ in the configuration space $\{0,1\}^{\otimes L}$, one can define a stationary state vector

$$|P\rangle_{\rightarrow}=Z_L^{-1}\langle\langle W|A^{\otimes L}|V\rangle\rangle \tag{1.4}$$

such that

$$\langle\tau_1,\tau_2,\ldots,\tau_L|P\rangle_{\rightarrow}=P_{\rightarrow}(\tau_1,\tau_2,\ldots,\tau_L). \tag{1.5}$$

Here the vectors $\langle\tau_1,\tau_2,\ldots,\tau_L|$ form an orthonormal basis in the space dual to the configuration space, i.e., $\langle\tau'|\tau\rangle=\delta_{\tau',\tau}$. The direct product $\otimes$ in Eq. (1.4) is taken over the one-site configuration spaces, spanned by the vectors (1.2). Therefore, the matrix $A^{\otimes L}$ is considered as a 2^L component column vector in the configuration space, each component of which represents a usual matrix product of L cofactors E and/or D. The symbol $\langle\langle W|\cdots|V\rangle\rangle$ denotes the vector obtained by applying the scalar product $\langle W|\cdots|V\rangle$ to each component of $A^{\otimes L}$. The normalization constant Z_L in Eq. (1.4) can be written as

$$Z_L=\langle W|C^L|V\rangle,\quad C\equiv E+D. \tag{1.6}$$

The master equation for the stationary state $|P\rangle_{\rightarrow}$ now takes the form, $|P\rangle_{\rightarrow}=\mathbf{T}_{\rightarrow}|P\rangle_{\rightarrow}$, where the transfer matrix $\mathbf{T}_{\rightarrow}$ has the following structure:

$$\mathbf{T}_{\rightarrow}=\mathbf{R}\mathbf{T}_{L-1,L}\cdots\mathbf{T}_{2,3}\mathbf{T}_{1,2}\mathbf{L}. \tag{1.7}$$

Here the matrices $\mathbf{L}$ and $\mathbf{R}$ describe the boundary conditions. They are nondiagonal only in the one-site subspace of configurations of the first, respectively the last, site of the chain,

$$\mathbf{L}=\mathcal{L}\otimes\mathbf{1}\otimes\cdots\otimes\mathbf{1}\otimes\mathbf{1},$$

$$\mathbf{R}=\mathbf{1}\otimes\mathbf{1}\otimes\cdots\otimes\mathbf{1}\otimes\mathcal{R}. \tag{1.8}$$

By $\mathbf{1}$ we have denoted the 2×2 unit matrix. In the one-site basis (1.2) the boundary conditions are represented by the matrices

$$\mathcal{L}=\begin{pmatrix}1-\alpha & 0\\ \alpha & 1\end{pmatrix},\quad \mathcal{R}=\begin{pmatrix}1 & \beta\\ 0 & 1-\beta\end{pmatrix}. \tag{1.9}$$

The matrices $\mathbf{T}_{i,i+1}$, $i=1,2,\ldots,L-1$, describe the particle hopping between the pair of nearest-neighbor sites $(i,i+1)$; hence they are nondiagonal only in the corresponding two-site configuration space:

$$\mathbf{T}_{i,i+1}=\mathbf{1}\otimes\cdots\otimes\mathbf{1}\otimes\mathcal{T}_{i,i+1}\otimes\mathbf{1}\otimes\cdots\otimes\mathbf{1}. \tag{1.10}$$

In the basis formed by column vectors of the type $|\tau_i,\tau_{i+1}\rangle=|\tau_i\rangle\otimes|\tau_{i+1}\rangle$, see Eq. (1.2), the matrix $\mathcal{T}_{i,i+1}$ has the explicit representation

$$\mathcal{T}_{i,i+1}=\begin{pmatrix}1 & 0 & 0 & 0\\ 0 & 1 & p & 0\\ 0 & 0 & 1-p & 0\\ 0 & 0 & 0 & 1\end{pmatrix}, \tag{1.11}$$

where p is the hopping probability.

Matrix-product representation of the stationary state of the asymmetric simple-exclusion process (ASEP) with open boundaries and sequential (as well as sublattice-parallel) update has been constructed in [4], see also [5], on the basis of the canceling mechanism. The general importance of the latter for one-dimensional stochastic processes with nearest-neighbor interaction has been recognized in [6]. According to the canceling mechanism, the first (in our case the left) boundary interaction produces a defect, $\langle W|\mathcal{L}A=\langle W|\hat{A}$, $\hat{A}=\hat{E}|0\rangle+\hat{D}|1\rangle$, which is transported through the system by the sequential action of the particle-hopping matrices, $\mathcal{T}_{i,i+1}(\hat{A}\otimes A)=A\otimes\hat{A}$, until it reaches the opposite boundary where it disappears due to the boundary interaction, $\mathcal{R}\hat{A}|V\rangle=A|V\rangle$. Explicitly this leads to the following set of equations:

$$\begin{aligned}
&[E,\hat{E}]=[D,\hat{D}]=0,\\
&\hat{E}D+p\hat{D}E=E\hat{D},\\
&(1-p)\hat{D}E=D\hat{E},\\
&(1-\alpha)\langle W|E=\langle W|\hat{E},\\
&\langle W|(\alpha E+D)=\langle W|\hat{D},\\
&(1-\beta)\hat{D}|V\rangle=D|V\rangle,\\
&(\hat{E}+\beta\hat{D})|V\rangle=E|V\rangle
\end{aligned} \tag{1.12}$$

for the four unknown matrices E, $\hat{E}$, D, and $\hat{D}$, and the two unknown vectors, $\langle W|$ and $|V\rangle$. Rajewsky, Schadschneider, and Schreckenberg [4] have suggested a reduction of the number of unknown matrices by setting

$$\hat{E}=E+\lambda I,\quad \hat{D}=D-\lambda I, \tag{1.13}$$

where I is the identity matrix and λ is some real number. We choose $\lambda=-1$ and reduce the set (1.12) to one equation for the bulk algebra,

$$pDE=D+(1-p)E, \tag{1.14}$$

and two equations for the boundary conditions,

$$\begin{aligned}
&\langle W|E=\alpha^{-1}\langle W|,\\
&D|V\rangle=(\beta^{-1}-1)|V\rangle.
\end{aligned} \tag{1.15}$$

By taking into account that $\hat{C}=C$, where $\hat{C}=\hat{E}+\hat{D}$, standard arguments lead to expressions for the stationary current J_L and particle density $\rho_L(i)$ at site i,

$$J_L=Z_{L-1}/Z_L,$$

$$\rho_L(i)=Z_L^{-1}\langle W|C^{i-1}DC^{L-i}|V\rangle, \tag{1.16}$$

which have the same form as in the case of the DEHP algebra [1]. Here Z_L is defined by Eq. (1.6).

A crucial point of our further consideration is the existence of a nontrivial infinite-dimensional solution of Eqs. (1.14) and (1.15) under the choice of the vectors

$$|V\rangle=\begin{pmatrix}1\\0\\0\\\vdots\end{pmatrix},\quad \langle W|=|V\rangle^T=(1,0,0,\ldots). \tag{1.17}$$

Consider the infinite orthonormal basis $\{|e_1'\rangle,|e_2'\rangle,\ldots\}$ in the vector space $\mathcal{S}$, where $|e_k'\rangle$ are column vectors with coordinates $|e_k'\rangle_n=\delta_{k,n}$, $k,n=1,2,\ldots$. Let us start with the matrices D_3 and E_3 given by Eq. (36) in [1], which are chosen to satisfy the standard DHEP algebra $D_3E_3=D_3+E_3$, and the boundary conditions $D_3|V\rangle=\beta^{-1}|V\rangle$, $\langle W|E_3=\alpha^{-1}\langle W|$. By suitable rescaling of the operators, $D'=[(1-p)/p]D_3$, $E'=(1/p)E_3$, and redefinition of the parameters α, β that enter into D_3 and E_3,

$$\alpha\to\frac{\alpha}{p},\quad \beta\to\frac{\beta(1-p)}{(1-\beta)p},$$

we obtain the matrices

$$E'=\frac{1}{p}\begin{pmatrix}1+\xi d & 0 & 0 & 0 & \ldots\\ \sqrt{1-\xi\eta} & 1 & 0 & 0 & \ldots\\ 0 & 1 & 1 & 0 & \ldots\\ 0 & 0 & 1 & 1 & \ldots\\ \ldots & \ldots & \ldots & \ldots & \ldots\end{pmatrix} \tag{1.18}$$

and

$$D'=\frac{d^2}{p}\begin{pmatrix}1+\eta d^{-1} & \sqrt{1-\xi\eta} & 0 & 0 & \ldots\\ 0 & 1 & 1 & 0 & \ldots\\ 0 & 0 & 1 & 1 & \ldots\\ 0 & 0 & 0 & 1 & \ldots\\ \ldots & \ldots & \ldots & \ldots & \ldots\end{pmatrix}, \tag{1.19}$$

where

$$d=\sqrt{1-p},\quad \xi=\frac{p-\alpha}{\alpha d},\quad \eta=\frac{p-\beta}{\beta d}. \tag{1.20}$$

Obviously, E' and D' satisfy the bulk algebra (1.14) and boundary conditions (1.15).

The main idea of our method is to choose a suitable representation which renders a symmetric matrix for the operator $C=E+D$. Since the elements of the upper diagonal in D' are d^2 times the elements of the lower diagonal in E', this can be achieved by renormalization of the basis vectors. Indeed, in the new orthonormal basis $\{|e_1\rangle,|e_2\rangle,\ldots\}$, defined by

$$|e_k\rangle=d^{1-k}|e_k'\rangle,\quad \langle e_k|=d^{k-1}\langle e_k'|,\quad k=1,2,\ldots, \tag{1.21}$$

the diagonal elements of any tridiagonal matrix A remain unchanged, while its nonzero off-diagonal elements change according to

$$\langle e_k|A|e_{k+1}\rangle=d^{-1}\langle e_k'|A|e_{k+1}'\rangle,$$

$$\langle e_{k+1}|A|e_k\rangle=d\langle e_{k+1}'|A|e_k'\rangle. \tag{1.22}$$

Thus E' and D' are transformed to

$$E=\frac{d}{p}\begin{pmatrix}d^{-1}+\xi & 0 & 0 & 0 & \ldots\\ \sqrt{1-\xi\eta} & d^{-1} & 0 & 0 & \ldots\\ 0 & 1 & d^{-1} & 0 & \ldots\\ 0 & 0 & 1 & d^{-1} & \ldots\\ \ldots & \ldots & \ldots & \ldots & \ldots\end{pmatrix} \tag{1.23}$$

and

$$D=\frac{d}{p}\begin{pmatrix}d+\eta & \sqrt{1-\xi\eta} & 0 & 0 & \ldots\\ 0 & d & 1 & 0 & \ldots\\ 0 & 0 & d & 1 & \ldots\\ 0 & 0 & 0 & d & \ldots\\ \ldots & \ldots & \ldots & \ldots & \ldots\end{pmatrix}. \tag{1.24}$$

Hence, the lattice ''translation operator'' C [7] is represented by the symmetric infinite-dimensional matrix

$$C\equiv E+D=\frac{d}{p}\begin{pmatrix}a+\xi+\eta & \sqrt{1-\xi\eta} & 0 & 0 & \ldots\\ \sqrt{1-\xi\eta} & a & 1 & 0 & \ldots\\ 0 & 1 & a & 1 & \ldots\\ 0 & 0 & 1 & a & \ldots\\ \ldots & \ldots & \ldots & \ldots & \ldots\end{pmatrix}, \tag{1.25}$$

where

$$a=d+d^{-1}=\frac{2-p}{\sqrt{1-p}}. \tag{1.26}$$

Now it is obvious that due to the choice of the vectors $|V\rangle$ and $\langle W|$ the quantities of interest J_L and $\rho_L(i)$, see Eqs. (1.6) and (1.16), depend on the elements of the matrices D and C only in the first $[L/2]+1$ rows and columns ($[x]$ denotes the entire part of $x\geqslant 0$). Therefore, for any finite L and a sufficiently large integer M, $M\geqslant[L/2]+1$, we can use a trun-

cated M-dimensional representation of the matrices and vectors involved (distinguished by the subscript M). After performing the calculations, we lift the truncation by letting its dimensionality go to infinity. In the limit $M\to\infty$ the results become exact for any size of the chain. Since the matrix C_M is (real or complex) symmetric, and, as it will be shown below, with real nondegenerate spectrum, it can be diagonalized by a similarity transformation with an orthogonal matrix U_M. This makes possible the explicit calculation of the relevant scalar products.

$$C_M(\xi,\eta)=\frac{d}{p}\begin{pmatrix} a+\xi+\eta & \sqrt{1-\xi\eta} & 0 & 0 & \dots & \dots \\ \sqrt{1-\xi\eta} & a & 1 & 0 & \dots & \dots \\ 0 & 1 & a & 1 & \dots & \dots \\ \dots & \dots & \dots & \dots & \dots & \dots \\ \dots & \dots & \dots & \dots & a & 1 \\ \dots & \dots & \dots & \dots & 1 & a \end{pmatrix} \tag{2.1}$$

and let $|V_M\rangle$ and $\langle W_M|$ be the M-component column and row vectors obtained by truncation of the vectors (1.17), respectively.

The eigenvalue problem for the symmetric matrix (2.1) can be solved by using a method similar to the one described in [8]. Let $\lambda_M(k)$, $k=1,\dots,M$, be the eigenvalues of $C_M(\xi,\eta)$. For $p\neq 0,1$ it is convenient to set

$$\lambda=(d/p)(a+2x) \tag{2.2}$$

and write the secular equation for the matrix $C_M(\xi,\eta)$ in the form

$$\det[C_M(\xi,\eta)-\lambda I_M]\equiv\left(\frac{d}{p}\right)^M[(\xi+\eta-2x)P_{M-1}(x) -(1-\xi\eta)P_{M-2}(x)]=0, \tag{2.3}$$

where $P_M(x)$ is the polynomial in x of degree M defined as

$$P_M(x)\equiv\det[(p/d)C_M(0,0)-(a+2x)I_M]. \tag{2.4}$$

Since the matrix $(p/d)C_M(0,0)$ has eigenvalues $a+2\cos[\pi k/(M+1)]$, $k=0,\dots,M$, one can readily show that

$$P_M(x)=2^M\prod_{k=1}^{M}\{\cos[\pi k/(M+1)]-x\}=(-1)^M U_M(x), \tag{2.5}$$

where $U_n(x)$ is the Chebyshev polynomial of the second kind. With the aid of the recurrence relationship $U_{n+1}(x)-2xU_n(x)+U_{n-1}(x)=0$, the secular equation (2.3) can be cast in the form

$$(1-\xi\eta)U_M(x)+(2x\xi\eta-\xi-\eta)U_{M-1}(x)=0. \tag{2.6}$$

It is convenient to substitute the variable x by a new variable ϕ

II. SPECTRAL PROPERTIES OF THE TRUNCATED PROPAGATOR

Let C_M be the $M\times M$ matrix obtained by truncation of Eq. (1.25) up to the Mth row and column:

$$x=\begin{cases}\cos\phi, & |x|\leqslant 1\\ \cosh\phi, & |x|\geqslant 1,\end{cases} \tag{2.7}$$

which leads to the representation

$$U_M(x)=\begin{cases}\sin[(M+1)\phi]/\sin\phi, & |x|\leqslant 1\\ \sinh[(M+1)\phi]/\sinh\phi, & |x|\geqslant 1.\end{cases} \tag{2.8}$$

Assuming first that $|x|\leqslant 1$ and $\xi\eta\neq 1$, we rewrite Eq. (2.6) as an equation for the unknown variable ϕ

$$\frac{\sin[(M+1)\phi]}{\sin(M\phi)}=\frac{\xi+\eta-2\xi\eta\cos\phi}{1-\xi\eta}\equiv f_R(\phi;\xi,\eta). \tag{2.9}$$

Due to Eq. (2.7) we need to consider only the roots in the interval $\phi\in[0,\pi]$. Note that when the probabilities α, β take values in the interval (0,1), then the parameters ξ, η range in the interval $(-d,+\infty)$. One can readily see that the number of real-valued solutions of Eq. (2.9) depends on the values of ξ and η (or p, α, and β). Obviously, the case $\xi\eta=1$, which in terms of p, α, and β reads

$$(1-\alpha)(1-\beta)=1-p, \tag{2.10}$$

defines a special line in the parameter space – this is the line on which the mean field approximation becomes exact. A remarkable feature of the spectral problem on the mean field line is that it has an exact and simple explicit solution. Thus, for $\eta=\xi^{-1}$ Eq. (2.6) has the obvious root $x=\cosh\xi$ which yields the largest eigenvalue of the mean field matrix $C_M^{\rm mf}(\xi)\equiv C_M(\xi,\xi^{-1})$:

$$\lambda_M^{\rm mf}(1)=(d/p)(a+\xi+\xi^{-1}). \tag{2.11}$$

For $\xi\neq 1$ this eigenvalue singles out from the rest of the spectrum given by the $M-1$ zeroes of $U_{M-1}(x)$:

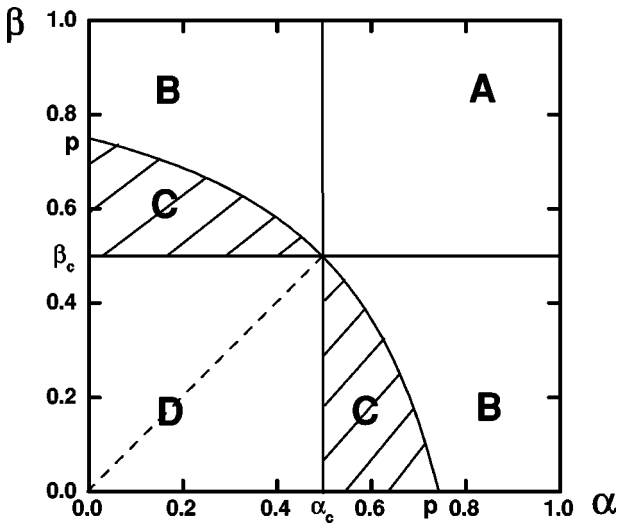

FIG. 1. The phase diagram in the α-β plane for $p=0.75$. Regions A, B, C, and D are distinguished by different spectral properties of the matrix C_M. The maximum-current phase occurs in region A. Regions B, C, and D correspond to the low-density phase for $\alpha<\beta$ and the high-density phase for $\alpha>\beta$; the coexistence line $\alpha=\beta$ in region D is shown by dashed line. The curved solid line is the mean-field line $(1-\alpha)(1-\beta)=1-p$.

$$\lambda_M^{\mathrm{mf}}(k)=(d/p)\left[a+2\cos\frac{\pi(k-1)}{M}\right],\quad k=2,\ldots,M. \tag{2.12}$$

The eigenvector of $C_M^{\mathrm{mf}}(\xi)$ corresponding to the largest eigenvalue (2.11) has the components

$$|u_M^{\mathrm{mf}}(1)\rangle_1\equiv u_M^{\mathrm{mf}}(1,1)=1,\quad |u_M^{\mathrm{mf}}(1)\rangle_l\equiv u_M^{\mathrm{mf}}(l,1)=0,$$

$$\text{for}\quad l=2,\ldots,M, \tag{2.13}$$

and the remaining eigenvectors $|u_M^{\mathrm{mf}}(k)\rangle$, $k=2,\ldots,M$, with eigenvalues (2.12), are given by

$$|u_M^{\mathrm{mf}}(k)\rangle_1\equiv u_M^{\mathrm{mf}}(1,k)=0,$$

$$|u_M^{\mathrm{mf}}(k)\rangle_l\equiv u_M^{\mathrm{mf}}(l,k)=\sqrt{\frac{2}{M}}\sin\frac{\pi(M+1-l)(k-1)}{M}$$

$$\text{for}\quad l=2,\ldots,M. \tag{2.14}$$

Two other special lines in the space of parameters are defined by the equations

$$\alpha=\alpha_c\equiv 1-\sqrt{1-p},\quad \beta=\beta_c\equiv 1-\sqrt{1-p}, \tag{2.15}$$

which correspond to $\xi=1$ and $\eta=1$, respectively. The analysis of the secular equation (2.9) shows that there are four regions in the square $\alpha,\beta\in[0,1]^2$, see Fig. 1, distinguished by different sets of eigenvalues and eigenvectors. Below we consider these four regions separately. For the sake of simplicity, in the remainder we omit the explicit dependence on the parameters p, ξ, and η (or p, α, and β) from the notation of the matrix C_M, its eigenvalues and eigenvectors. The eigenvalues are labeled in the order of decreasing magnitude.

A. Region A: $\alpha_c<\alpha\leqslant 1$ and $\beta_c<\beta\leqslant 1$

In terms of ξ and η this region is defined by $-\sqrt{1-p}\leqslant\xi<1$ and $-\sqrt{1-p}\leqslant\eta<1$. Since then the right-hand side of Eq. (2.9) is a monotonic function of ϕ, ranging between $f(0;\xi,\eta)<1$ and $f(\pi;\xi,\eta)>-1$; for sufficiently large M this equation has exactly M simple real roots $\phi_M(k)$, $k=1,\ldots,M$, in the interval $(0,\pi)$; see Fig. 2. These roots satisfy the inequalities

$$\pi(k-1)/M<\phi_M(k)<\pi k/M,\quad k=1,\ldots,M. \tag{2.16}$$

According to Eqs. (2.2) and (2.7), the eigenvalues of the matrix C_M are

$$\lambda_M(k)=(d/p)[a+2\cos\phi_M(k)],\quad k=1,\ldots,M. \tag{2.17}$$

A complete set of orthonormal eigenvectors of C_M is given by the column vectors $|u_M(k)\rangle$, $k=1,\ldots,M$, with components

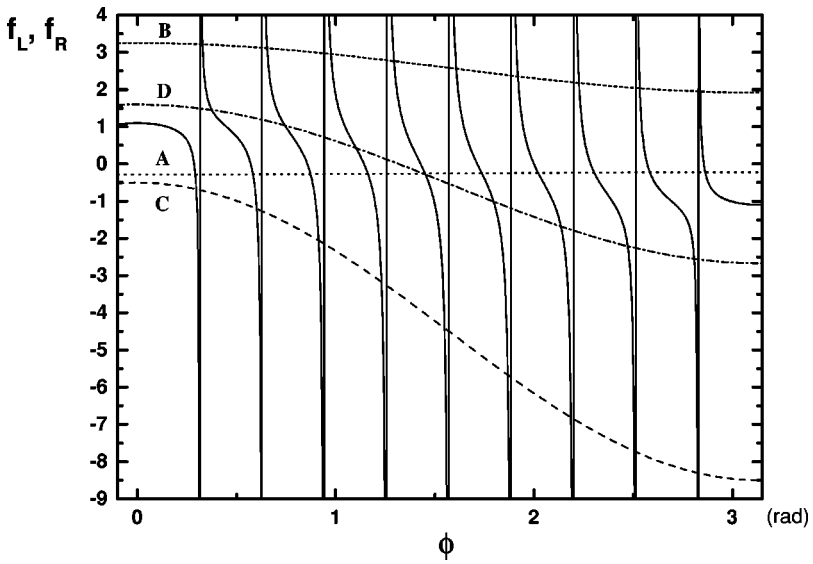

FIG. 2. The behavior of the left-hand side f_L (solid line) and the right-hand side f_R (different broken lines) of Eq. (2.9) at $M=10$ is shown as a function of ϕ. The broken lines depicting f_R are: dotted (region A), short-dashed (region B), dashed (region C), and dashed-dotted (region D).

$$|u_M(k)\rangle_1 \equiv u_M(1,k) = b_M(k)\frac{\sin[M\phi_M(k)]}{\sqrt{1-\xi\eta}},$$

$$|u_M(k)\rangle_l \equiv u_M(l,k) = b_M(k)\sin[(M+1-l)\phi_M(k)] \quad \text{for} \quad l=2,\ldots,M, \tag{2.18}$$

where $b_M(k)$ is the normalization constant

$$b_M(k) = 2^{1/2}\left\{ M + [1+\xi\eta-(\xi+\eta) \times\cos\phi_M(k)]\frac{\sin^2[M\phi_M(k)]}{(1-\xi\eta)\sin^2\phi_M(k)}\right\}^{-1/2}. \tag{2.19}$$

Since $\phi_M(k)$ satisfies Eq. (2.9), we have

$$\tan[M\phi_M(k)] = \frac{(1-\xi\eta)\sin\phi_M(k)}{\xi+\eta-(1+\xi\eta)\cos\phi_M(k)}, \tag{2.20}$$

and from inequalities (2.16) it follows that

$$\sin[M\phi_M(k)] = \frac{(-1)^{k-1}|(1-\xi\eta)\sin\phi_M(k)|}{[1-2\xi\cos\phi_M(k)+\xi^2]^{1/2}[1-2\eta\cos\phi_M(k)+\eta^2]^{1/2}}. \tag{2.21}$$

With the aid of the above equalities, the normalization constant (2.19) can be written as

$$b_M(k) = 2^{1/2}\left\{ M + \frac{(1-\xi\eta)[1+\xi\eta-(\xi+\eta)\cos\phi_M(k)]}{[1-2\xi\cos\phi_M(k)+\xi^2][1-2\eta\cos\phi_M(k)+\eta^2]}\right\}^{-1/2}. \tag{2.22}$$

Equations (2.21) and (2.22) are convenient for taking the limit $M\to\infty$.

Thus, the real symmetric matrix C_M is diagonalized by the similarity transformation

$$\tilde{C}_M \equiv U_M^{-1}C_M U_M = \begin{pmatrix} \lambda_M(1) & 0 & \ldots & 0 \\ 0 & \lambda_M(2) & \ldots & 0 \\ \ldots & \ldots & \ldots & \ldots \\ 0 & 0 & \ldots & \lambda_M(M) \end{pmatrix}, \tag{2.23}$$

where U_M is the real orthogonal matrix with elements $(U_M)_{l,k} = u_M(l,k)$, $l,k=1,\ldots,M$, and $U_M^{-1} = U_M^T$, the transposed of U_M.

B. Region B: $(1-\alpha)(1-\beta)<1-p$ and $\alpha<\alpha_c$ or $\beta<\beta_c$

In this region $\xi\eta<1$ and either $\xi>1$ and $-\sqrt{1-p}\leqslant\eta<\xi^{-1}$, or $\eta>1$ and $-\sqrt{1-p}\leqslant\xi<\eta^{-1}$. Since $f_R(0;\xi,\eta)>1$ and $f_R(\pi;\xi,\eta)>-1$, for sufficiently large M Eq. (2.9) has $M-1$ simple real roots $\phi_M(k)$, $k=2,\ldots,M$, in the interval $(0,\pi)$; see Fig. 2. These roots satisfy inequalities (2.16). The missing eigenvalue of C_M is provided by the pair of complex conjugate imaginary solutions $\phi=\pm i\phi_M(1)$ of Eq. (2.9) or, equivalently, by the pair of real solutions $\phi=\pm\phi_M(1)$ of the equation

$$\frac{\sinh[(M+1)\phi]}{\sinh(M\phi)} = \frac{\xi+\eta-2\xi\eta\cosh\phi}{1-\xi\eta} \equiv f_R(i\phi;\xi,\eta) \tag{2.24}$$

which follows from Eqs. (2.6) and (2.8) when $|x|\geqslant 1$. Note that for $\phi\geqslant 0$ the left-hand side of the above equation is a monotonically increasing function of ϕ with a minimum $1+M^{-1}$ at $\phi=0$, while the right-hand side is a monotonically decreasing function of ϕ with a maximum at $\phi=0$,

$$f_R(0;\xi,\eta) = \frac{\xi+\eta-2\xi\eta}{1-\xi\eta} > 1. \tag{2.25}$$

Hence, for large enough M there is a unique positive solution of Eq. (2.24); see Fig. 3. Its asymptotic form as $M\to\infty$ at fixed $\xi>1$ and $\eta<\xi^{-1}$ is

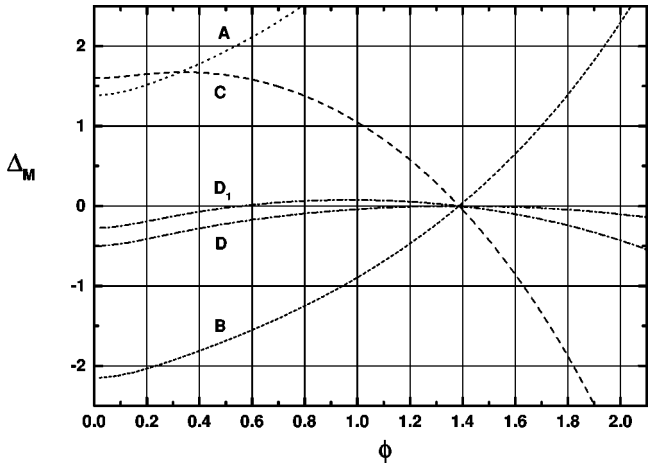

FIG. 3. The behavior of the difference Δ_M between the left-hand side f_L and the right-hand side f_R of Eq. (2.24) at $M=10$, as a function of the dimenshionless argument ϕ. The lines are labeled according to the regions: dotted (region A), short-dashed (region B), dashed (region C), and dashed-dotted (region D); the latter case is represented by two lines: at a symmetric (line D), and asymmetric (line D_1) point in region D.

$$\phi_M(1)=\ln\xi-\frac{(\xi-\xi^{-1})(1-\xi\eta)}{\xi-\eta}\,\xi^{-2M}+O(\xi^{-4M}). \tag{2.26}$$

In the case when $\eta>1$ and $\xi<\eta^{-1}$ the asymptotic form of $\phi_M(1)$ as $M\to\infty$ follows from Eq. (2.26) by exchanging places of ξ and η.

It is easily seen that $\phi=\phi_M(1)$ yields the largest eigenvalue of the matrix C_M,

$$\lambda_M(1)=(d/p)[a+2\cosh\phi_M(1)], \tag{2.27}$$

which singles out from the rest of the spectrum. The remaining $M-1$ eigenvalues are given by Eq. (2.17) with $\phi_M(k)$, $k=2,\ldots,M$, satisfying Eq. (2.9). The eigenvector of the matrix C_M with eigenvalue (2.27) is the column vector $|u_M(1)\rangle$ with components

$$|u_M(1)\rangle_1\equiv u_M(1,1)=b_M(1)\frac{\sinh[M\phi_M(1)]}{\sqrt{1-\xi\eta}}\quad\text{for}\quad l=1,$$

$$|u_M(1)\rangle_l\equiv u_M(l,1)=b_M(1)\sinh[(M+1-l)\phi_M(1)]\quad\text{for}\quad l=2,\ldots,M, \tag{2.28}$$

where the normalization constant

$$b_M(1)=2^{1/2}\left\{[(\xi+\eta)\cosh\phi_M(1)-1-\xi\eta]\times\frac{\sinh^2[M\phi_M(1)]}{(1-\xi\eta)\sinh^2\phi_M(1)}-M\right\}^{-1/2} \tag{2.29}$$

is the analytical continuation to imaginary $\phi_M(1)$ of expression (2.19) at $k=1$. One can readily check that on approaching the line $\xi\eta=1$ from region B the eigenvalues and eigenvectors of $C_M(\xi,\eta)$ tend to the corresponding eigenvalues $\lambda_M^{\rm mf}(k)$ and eigenvectors $|u_M^{\rm mf}(k)\rangle$ of the mean field matrix $C_M^{\rm mf}(\xi)=C_M(\xi,\xi^{-1})$, see Eqs. (2.11)–(2.14).

Note that as a direct consequence of Eq. (2.24) one obtains the equalities; compare with Eqs. (2.20) and (2.21),

$$\tanh[M\phi_M(1)]=\frac{(1-\xi\eta)\sinh\phi_M(1)}{\xi+\eta-(1+\xi\eta)\cosh\phi_M(1)}, \tag{2.30}$$

and

$$\sinh[M\phi_M(1)]=\frac{|1-\xi\eta|\sinh\phi_M(1)}{[2\xi\cosh\phi_M(1)-1-\xi^2]^{1/2}[2\eta\cosh\phi_M(1)-1-\eta^2]^{1/2}}. \tag{2.31}$$

Thus, in region B the real symmetric matrix C_M is diagonalized by the similarity transformation (2.23), where the first column of the real orthogonal matrix U_M is given by Eq. (2.28), and the remaining columns $k=2,\ldots,M$, have components of the form (2.18).

C. Region C: $(1-\alpha)(1-\beta)>1-p$ and $\alpha>\alpha_c$ or $\beta>\beta_c$

In this region $\xi\eta>1$ and either $\xi>1$ and $\xi^{-1}<\eta<1$, or $\eta>1$ and $\eta^{-1}<\xi<1$. Now the off-diagonal elements $(C_M)_{1,2}=(C_M)_{1,2}=\mathrm{i}\sqrt{\xi\eta-1}$, see Eq. (2.1), are imaginary. Nevertheless, the coefficients in the secular equation (2.6) are real, since they depend only on the product of the above matrix elements. Therefore, after substitution (2.7), the equation for the spectrum of C_M takes again one of the forms (2.9) or (2.24). Since $f_R(0;\xi,\eta)<1$ and $f_R(\pi;\xi,\eta)<-1$, for sufficiently large M Eq. (2.9) has $M-1$ simple real roots $\phi_M(k)$, $\pi(k-2)/M<\phi_M(k)<\pi(k-1)/M$, $k=2,\ldots,M$; see Fig. 2. The missing eigenvalue of C_M is provided by the pair of real solutions $\phi=\pm\phi_M(1)$ of Eq. (2.24). To show that for large enough M this equation has a unique positive solution, we consider the difference, see Fig. 3,

$$\Delta_M(\phi;\xi,\eta)\equiv\frac{\sinh[(M+1)\phi]}{\sinh(M\phi)}-\frac{2\xi\eta\cosh\phi-\xi-\eta}{\xi\eta-1}$$

$$=-\frac{e^{\phi}+\xi\eta e^{-\phi}-\xi-\eta}{\xi\eta-1}+[\coth(M\phi)-1]\sinh\phi. \tag{2.32}$$

The $M\to\infty$ limit function $\Delta_\infty(\phi;\xi,\eta)$ first increases from a positive value at $\phi=0$, attains maximum at $\phi=\ln\sqrt{\xi\eta}$, then monotonically decreases crossing the abscissa at $\phi=\ln(\max\{\xi,\eta\})$ and tending to $-\infty$ like $-(\xi\eta-1)^{-1}\exp\phi$ as $\phi\to\infty$. The perturbative solution of Eq. (2.24) as $M\to\infty$ at fixed $\xi>1$ and $\xi^{-1}<\eta<1$ yields

$$\phi_M(1)=\ln\xi+\frac{(\xi-\xi^{-1})(\xi\eta-1)}{\xi-\eta}\,\xi^{-2M}+O(\xi^{-4M}). \tag{2.33}$$

In the case when $\eta>1$ and $\eta^{-1}<\xi<1$ the asymptotic form of $\phi_M(1)$ follows by exchanging places of ξ and η in Eq. (2.33). As it is readily seen by comparison with Eq. (2.26), $\phi_M(1)$ has the same analytical form in regions B and C. The largest eigenvalue of the matrix C_M is given by Eq. (2.27); the remaining $M-1$ eigenvalues have the form (2.17), where $\phi_M(k)$, $k=2,\ldots,M$, are the solutions of Eq. (2.9).

The eigenvector of the matrix C_M which corresponds to the largest eigenvalue (2.27) can be obtained by analytical continuation of Eq. (2.28) from $\xi\eta<1$ in region B to $\xi\eta>1$ in region C. At that we take into account that the normalization constant (2.29) passes through zero on crossing the mean field line $\xi\eta=1$, and becomes imaginary in region C. As a result we obtain the column vector $|u_M(1)\rangle$ with components

$$|u_M(1)\rangle_1 \equiv u_M(1,1) = b_M(1)\frac{\sinh[M\phi_M(1)]}{\sqrt{\xi\eta-1}},$$

$$|u_M(1)\rangle_l \equiv u_M(l,1) = \mathrm{i}\, b_M(1)\sinh[(M+1-l)\phi_M(1)]$$

$$\text{for } \; l=2,\ldots,M. \tag{2.34}$$

Here the constant $b_M(1)$ is given by, compare with Eq. (2.29),

$$b_M(1) = 2^{1/2}\left\{[(\xi+\eta)\cosh\phi_M(1) - 1 - \xi\eta] \times \frac{\sinh^2[M\phi_M(1)]}{(\xi\eta-1)\sinh^2\phi_M(1)} + M\right\}^{-1/2}, \tag{2.35}$$

where $(\xi+\eta)\cosh\phi_M(1) - 1 - \xi\eta > 0$.

The remaining eigenvalues $\lambda_M(k)$, $k=2,\ldots,M$, are of the form (2.17), and the corresponding eigenvectors are given by the analytical continuation of Eq. (2.18) across the mean field line:

$$|u_M(k)\rangle_1 \equiv u_M(1,k) = b_M(k)\frac{-\mathrm{i}\sin[M\phi_M(k)]}{\sqrt{\xi\eta-1}},$$

$$|u_M(k)\rangle_l \equiv u_M(l,k) = b_M(k)\sin[(M+1-l)\phi_M(k)]$$

$$\text{for } \; l=2,\ldots,M. \tag{2.36}$$

Here the constant $b_M(k)$ is given by expression (2.22), as it is in regions A and B.

The diagonalization problem for the matrix C_M in regions C and D (see below) differs in one essential aspect from that in regions A and B: for $\xi\eta > 1$ the matrix C_M is complex symmetric, with $(C_M)_{1,2} = (C_M)_{2,1} = \mathrm{i}\sqrt{\xi\eta-1}$, and not Hermitian (or real symmetric). Due to $C_M^\dagger C_M \neq C_M C_M^\dagger$, the matrix C_M cannot be diagonalized by means of unitary transformation. However, since C_M has a simple real-valued spectrum, the similarity transformation (2.23) with the complex orthogonal matrix U_M, $U_M^{-1} = U_M^T$, the elements of which $(U_M)_{l,k} = u_M(l,k)$, $l,k=1,\ldots,M$, are defined in Eqs. (2.34) and (2.36), brings it to a diagonal form. Due to $U_M^{-1} \neq U_M^\dagger$, the normalization constants $b_M(k)$ of the eigenvectors $|u_M(k)\rangle$, $k=1,\ldots,M$, do not equal their reciprocal norm but are determined from the condition $U_M^T U_M = I_M$.

D. Region D: $\alpha < \alpha_c$ and $\beta < \beta_c$

In this region $\xi > 1$ and $\eta > 1$. The essential difference from the previous case is that now both $f_R(\phi;\xi,\eta) > 1$ and $f_R(\pi;\xi,\eta) < -1$, so that for sufficiently large M Eq. (2.9) has $M-2$ simple real roots $\phi_M(k)$, $k=3,\ldots,M$, in the interval $(0,\pi)$, see Fig. 2. The two missing eigenvalues of C_M are given by the positive solutions $\phi = \phi_M(k)$ with $k=1,2$ of equation (2.24). Indeed, in this region the limit function $\Delta_\infty(\phi;\xi,\eta)$, see Eq. (2.32), begins to increase from a *negative* value at $\phi=0$, attains a *positive* maximum at $\phi = \ln\sqrt{\xi\eta}$, and then monotonically decreases to $-\infty$ as $\phi \to \infty$. Thus, it crosses the abscissa at two positive values: $\phi = \ln\xi$ and $\phi = \ln\eta$; the behavior of $\Delta_M(\phi;\xi,\eta)$ for large M is shown in Fig. 3. A perturbative expansion of Eq. (2.24) as $M\to\infty$ at fixed $\xi > \eta > 1$ yields the roots

$$\phi_M(1) = \ln\xi + \frac{(\xi-\xi^{-1})(\xi\eta-1)}{\xi-\eta}\xi^{-2M} + O(\xi^{-4M}) \tag{2.37}$$

and

$$\phi_M(2) = \ln\eta - \frac{(\eta-\eta^{-1})(\xi\eta-1)}{\xi-\eta}\eta^{-2M} + O(\eta^{-4M}). \tag{2.38}$$

Note that $\phi_M(1)$ has the same analytical form as in region C, see Eq. (2.33).

The case $\xi = \eta > 1$ is a special one, since then the two roots

$$\phi_M(1) = \ln\xi + (\xi-\xi^{-1})\xi^{-M} + O(\xi^{-2M}),$$

$$\phi_M(2) = \ln\xi - (\xi-\xi^{-1})\xi^{-M} + O(\xi^{-2M}) \tag{2.39}$$

become degenerate in the limit $M\to\infty$.

Now there are two large eigenvalues of the matrix C_M,

$$\lambda_M(k) = (d/p)[a + 2\cosh\phi_M(k)] \quad k=1,2, \tag{2.40}$$

which split off from the rest of the spectrum. The remaining $M-2$ eigenvalues have the form (2.17), where $\phi_M(k)$, $\pi(k-2)/M < \phi_M(k) < \pi(k-1)/M$, $k=3,\ldots,M$, are the solutions of Eq. (2.9).

To obtain the eigenvectors $|u_M(k)\rangle$, $k=1,2$, of the matrix C_M with the two largest eigenvalues (2.40) by analytical continuation from region C, we take into account that for $\xi \geqslant \eta > 1$ one has

$$(\xi+\eta)\cosh\phi_M(1) - 1 - \xi\eta > 0 > (\xi+\eta)\cosh\phi_M(2) - 1 - \xi\eta. \tag{2.41}$$

Therefore, the normalization constant $b_M(1)$ is defined by the same expression (2.35) as in region C, and the components of the eigenvector $|u_M(1)\rangle$ are given by Eq. (2.34). Since the right-hand side of Eq. (2.35) with $\phi_M(1)$ replaced by $\phi_M(2)$ becomes imaginary, the components of the eigenvector $|u_M(2)\rangle$ are

$$|u_M(2)\rangle_1 \equiv u_M(1,2) = b_M(2)\frac{\mathrm{i}\sinh[M\phi_M(2)]}{\sqrt{\xi\eta-1}},$$

$$|u_M(2)\rangle_l \equiv u_M(l,2) = -b_M(2)\sinh[(M+1-l)\phi_M(2)]$$

$$\text{for } \; l=2,\ldots,M, \tag{2.42}$$

where the normalization constant $b_M(2)$ is

$$b_M(2) = 2^{1/2}\left\{[1+\xi\eta-(\xi+\eta)\cosh\phi_M(2)] \times \frac{\sinh^2[M\phi_M(2)]}{(\xi\eta-1)\sinh^2\phi_M(2)} - M\right\}^{-1/2}. \tag{2.43}$$

The remaining eigenvectors $|u_M(k)\rangle$, $k=3,\ldots,M$, have the same analytical form as in region C, see (2.36), with constant $b_M(k)$ given by Eq. (2.22). It should be noted that at large but finite M the eigenvalue $\lambda_M(2)$ and eigenvector $|u_M(2)\rangle$ defined in region C preserve their analytical form in a $O(M^{-1})$ neighborhood of the boundary line between C and D, on the side of region D. For example, the solution for $\phi_M(2)$ of Eq. (2.9) is real positive for $0 \leqslant \eta-1<\epsilon_M(\xi)$, $\xi>1$, where $\epsilon_M(\xi)=[M-\xi/(\xi-1)]^{-1}$ vanishes at $\eta=1+\epsilon_M(\xi)$ and becomes imaginary for $\eta>1+\epsilon_M(\xi)$ when the next to the largest solution of Eq. (2.24) emerges.

As in region C, the complex symmetric matrix C_M in region D is diagonalized by the similarity transformation (2.23), where the components in the first and the second columns of the complex orthogonal matrix U_M are defined in Eqs. (2.34) and (2.42), respectively, while the remaining $M-2$ columns ($k=3,\ldots,M$) are given by Eq. (2.36).

E. Summary

Here we summarize the qualitative features of the spectrum of the truncated propagator matrix C_M at large M in the four regions of the parameter space shown in Fig. 1.

(1) Everywhere the spectrum is real and nondegenerate; it is a symmetric function of the parameters ξ and η. The eigenvectors are real in regions A and B, and some of their components are imaginary in regions C and D. In the whole space of parameters the normalization condition is $\Sigma_{l=1}^{M} u_M^2(l,k)=1$, $k=1,\ldots,M$.

(2) In region A the spectrum fills with uniform density the interval from $(d/p)(a-2)$ to $(d/p)(a+2)$, and becomes quasicontinuous in the limit $M\to\infty$.

(3) In regions B, C, and D the largest eigenvalue $\lambda_M(1)$ splits from the ''quasicontinuous'' part of the spectrum; in region D so does also the next-to-the-largest eigenvalue $\lambda_M(2)$.

(4) The spectra in regions B, C, and D, excluding the line $\xi\neq\eta$ in region D, have an important feature in common with the mean field case ($\xi\eta=1$): except at the point $(\xi,\eta)=(1,1)$, the whole spectrum is dominated by the single largest eigenvalue

$$\lambda_M(1)=\begin{cases}(d/p)(a+\xi+\xi^{-1})+O(\xi^{-M}) & \text{for } \xi>\eta\\ (d/p)(a+\eta+\eta^{-1})+O(\eta^{-M}) & \text{for } \eta>\xi,\end{cases} \tag{2.44}$$

which differs from the mean field one, see Eq. (2.11), only by exponentially small in M corrections. The point $(\xi,\eta)=(1,1)$ is a boundary point of all the four regions and belongs to the mean field line as well.

(5) On the line $\xi=\eta$ in region D the two largest eigenvalues become asymptotically (as $M\to\infty$) degenerate, see Eq. (2.39).

As is known [9], in the thermodynamic limit $M\to\infty$ region A corresponds to the *maximum current phase*; regions B, C, and D for $\xi>\eta$ ($\alpha<\beta$) belong to the *low-density phase*, and for $\xi<\eta$ ($\alpha>\beta$) belong to the *high-density phase*. The distinction between the latter three regions within a single phase is expected to affect more subtle characteristics like density profile, correlation functions, rate of approach to the thermodynamic limit, etc.

III. CALCULATION OF THE CURRENT

From Eq. (1.16) it is clear that the basic quantity we have to calculate is

$$Z_L(\xi,\eta)=\langle W|C^L|V\rangle=\langle W_M|C_M^L(\xi,\eta)|V_M\rangle, \tag{3.1}$$

where the last equality holds independently of M for all $M\geqslant[L/2]+1$. By applying the similarity transformation (2.23) of the matrix C_M, we obtain

$$\begin{aligned}Z_L(\xi,\eta)&=\langle W_M|U_M\tilde{C}_M(\xi,\eta)U_M^{-1}|V_M\rangle\\ &=\sum_{k=1}^{M}\lambda_M^L(k)u_M^2(1,k).\end{aligned} \tag{3.2}$$

In region A, from Eq. (2.17) for the eigenvalues $\lambda_M(k)$ and expressions (2.18), (2.22) for the components $u_M(1,k)$, by using the uniform distribution of $\phi_M(k)$, $k=1,\ldots,M$ over the interval $[0,\pi]$, see inequalities (2.16), we obtain in the limit $M\to\infty$ the following exact result ($\xi\neq\eta$):

$$Z_L^{\mathrm{A}}(\xi,\eta)=\left(\frac{d}{p}\right)^L\left[\frac{\xi}{\xi-\eta}I_L(\xi)+\frac{\eta}{\eta-\xi}I_L(\eta)\right], \tag{3.3}$$

where

$$I_L(\xi)=\frac{2}{\pi}\int_0^{\pi}\mathrm{d}\phi\,\frac{(a+2\cos\phi)^L\sin^2\phi}{1-2\xi\cos\phi+\xi^2}. \tag{3.4}$$

The result for $Z_L^{\mathrm{A}}(\xi,\xi)$, with $|\xi|<1$ in region A, can be obtained by taking the limit $\eta\to\xi$ in expression (3.3):

$$Z_L^{\mathrm{A}}(\xi,\xi)=\left(\frac{d}{p}\right)^L\left[I_L(\xi)+\xi\frac{\partial}{\partial\xi}I_L(\xi)\right]\equiv(d/p)^L(1-\xi^2)K_L(\xi), \tag{3.5}$$

where

$$K_L(\xi)=\frac{2}{\pi}\int_0^{\pi}\mathrm{d}\phi\,\frac{(a+2\cos\phi)^L\sin^2\phi}{(1-2\xi\cos\phi+\xi^2)^2}. \tag{3.6}$$

One can perform the integration in Eq. (3.4) for $|\xi|<1$ to obtain the finite sum

$$\begin{aligned}I_L(\xi)=S_L(\xi)\equiv\frac{a^L}{L+1}\Bigg[&\sum_{k=0}^{[L/2]}\binom{L+1}{2k+1}a^{-2k}\sum_{m=0}^{k}(2m+1)\\ &\times\binom{2k+1}{k-m}\xi^{2m}+\sum_{k=1}^{[(L+1)/2]}\binom{L+1}{2k}\\ &\times a^{-2k+1}\sum_{m=1}^{k}2m\binom{2k}{k-m}\xi^{2m-1}\Bigg].\end{aligned} \tag{3.7}$$

A similar representation for $K_L(\xi)$ follows from Eqs. (3.5) and (3.7). As expected, Eqs. (3.3) and (3.7) imply that $Z_L(\xi,\eta)$ is a polynomial symmetric in ξ and η.

In regions B and C one has to take into account the contribution of the single largest eigenvalue $\lambda_M(1)$, see Eq. (2.27), and in region D one has also to take into account the contribution of the next-to-the-largest eigenvalue $\lambda_M(2)$, see Eq. (2.40). The remaining part of the spectrum yields inte-

grals of the same analytical form as in region A, see Eqs. (3.3) and (3.4). From the explicit expressions for $u_M(1,1)$, given by Eqs. (2.28) and (2.29) in region B, and by Eqs. (2.34) and (2.35) in regions C and D, we obtain in the limit $M\to\infty$

$$\lim_{M\to\infty} u_M^2(1,1)=\begin{cases}(\xi-\xi^{-1})/(\xi-\eta) & \text{for } \xi>\eta\\ (\eta-\eta^{-1})/(\eta-\xi) & \text{for } \eta>\xi.\end{cases} \tag{3.8}$$

Similarly, from expressions (2.42) and (2.43) for $u_M(1,2)$ in region D we obtain

$$\lim_{M\to\infty} u_M^2(1,2)=\begin{cases}-(\eta-\eta^{-1})/(\xi-\eta), & \text{for } \xi>\eta\\ -(\xi-\xi^{-1})/(\eta-\xi) & \text{for } \eta>\xi.\end{cases} \tag{3.9}$$

Thus, by taking the limit $M\to\infty$ in regions B and C at $\xi>\eta$, we obtain the exact result

$$Z_L^{\mathrm{B,C}}(\xi,\eta)=\left(\frac{d}{p}\right)^L\frac{\xi-\xi^{-1}}{\xi-\eta}(a+\xi+\xi^{-1})^L+Z_L^{\mathrm{A}}(\xi,\eta). \tag{3.10}$$

The case $\eta>\xi$ follows from the above expression by exchanging places of ξ and η. Note that by using the identities

$$I_L(\xi>1)=\xi^{-2}I_L(\xi^{-1})=\xi^{-2}S_L(\xi^{-1}) \tag{3.11}$$

and

$$(a+\xi+\xi^{-1})^L(1-\xi^{-2})=S_L(\xi)-\xi^{-2}S_L(\xi^{-1}) \tag{3.12}$$

one can cast Eq. (3.10) in the form of exactly the same symmetric polynomial in ξ and η as in region A, namely,

$$Z_L^{\mathrm{B,C}}(\xi,\eta)=\left(\frac{d}{p}\right)^L\left[\frac{\xi}{\xi-\eta}S_L(\xi)+\frac{\eta}{\eta-\xi}S_L(\eta)\right]. \tag{3.13}$$

In a similar way, by taking the limit $M\to\infty$ in region D at $\xi\neq\eta$, we obtain

$$Z_L^{\mathrm{D}}(\xi,\eta)=\left(\frac{d}{p}\right)^L\left[\frac{\xi-\xi^{-1}}{\xi-\eta}(a+\xi+\xi^{-1})^L+\frac{\eta-\eta^{-1}}{\eta-\xi}\times(a+\eta+\eta^{-1})^L\right]+Z_L^{\mathrm{A}}(\xi,\eta). \tag{3.14}$$

Obviously, the above expression is a symmetric function of ξ and η. Since now both $\xi>1$ and $\eta>1$, the application of identities (3.11) and (3.12) brings Eq. (3.14) in the form of the polynomial (3.13).

Now we consider the limit $M\to\infty$ on the line $\xi=\eta$ in region D. Due to the asymptotic form (2.39) of $\phi_M(1)$ and $\phi_M(2)$, which leads to inequalities (2.41) taken at $\xi=\eta$, we obtain from Eq. (2.24)

$$\begin{aligned}\sinh[M\phi_M(1)]&=\frac{(\xi^2-1)\sinh\phi_M(1)}{2\xi\cosh\phi_M(1)-1-\xi^2},\\ \sinh[M\phi_M(2)]&=\frac{(\xi^2-1)\sinh\phi_M(2)}{1+\xi^2-2\xi\cosh\phi_M(2)}.\end{aligned} \tag{3.15}$$

From Eqs. (2.35) and (2.43) for the normalization constants $b_M(1)$ and $b_M(2)$, respectively, we obtain at $\xi=\eta$

$$\begin{aligned}b_M^2(1)&=2\left[\frac{\sinh[M\phi_M(1)]}{\sinh\phi_M(1)}+M\right]^{-1},\\ b_M^2(2)&=2\left[\frac{\sinh[M\phi_M(2)]}{\sinh\phi_M(2)}-M\right]^{-1}.\end{aligned} \tag{3.16}$$

Hence, it follows that at large M

$$\begin{aligned}u_M^2(1,1)&=\frac{\xi^M}{2\xi}+\frac{\xi+\xi^{-1}}{2\xi}+O(M\xi^{-M}),\\ u_M^2(1,2)&=-\frac{\xi^M}{2\xi}+\frac{\xi+\xi^{-1}}{2\xi}+O(M\xi^{-M}).\end{aligned} \tag{3.17}$$

Finally, by rewriting $Z_L^{\mathrm{D}}(\xi,\xi)$ indentically as

$$Z_L^{\mathrm{D}}(\xi,\xi)=\lambda_M^L(1)[u_M^2(1,1)+u_M^2(1,2)]-[\lambda_M^L(1)-\lambda_M^L(2)]u_M^2(1,2)+\sum_{k=3}^{M}\lambda_M^L(k)u_M^2(1,k), \tag{3.18}$$

and passing to the limit $M\to\infty$, we obtain

$$Z_L^{\mathrm{D}}(\xi,\xi)=\left(\frac{p}{d}\right)^L\left[\frac{L(\xi-\xi^{-1})^2}{\xi(a+\xi+\xi^{-1})}+1+\xi^{-2}\right](a+\xi+\xi^{-1})^L+Z_L^{\mathrm{A}}(\xi,\xi), \tag{3.19}$$

where $Z_L^{\mathrm{A}}(\xi,\xi)$ is defined in Eq. (3.5). Naturally, the same result follows by taking the limit $\eta\to\xi$ in Eq. (3.14).

A. Current in the maximum-current phase

The exact results for the current follow from Eq. (1.16) and the expressions for $Z_L(\xi,\eta)$ in region A. Thus, from Eq. (3.3) it follows that when $\xi\neq\eta$ the current equals the ratio of the symmetric in ξ and η polynomials

$$J_L(\xi,\eta)=\left(\frac{p}{d}\right)\frac{\xi S_{L-1}(\xi)-\eta S_{L-1}(\eta)}{\xi S_L(\xi)-\eta S_L(\eta)} \tag{3.20}$$

and for $\xi=\eta$ we obtain from Eq. (3.5)

$$J_L(\xi,\xi)=(p/d)K_{L-1}(\xi)/K_L(\xi). \tag{3.21}$$

The asymptotic expressions for the current at large L are most readily obtained by applying the Laplace method to the integral in Eq. (3.4):

$$I_L(\xi)=\frac{(a+2)^{L+3/2}}{2\sqrt{\pi}(1-\xi)^2}L^{-3/2}[1+O(L^{-1})],\quad |\xi|<1. \tag{3.22}$$

By substitution of this result in Eq. (3.3), we obtain the asymptotic form of $Z_L(\xi,\eta)$ for $\xi\neq\eta$

$$Z_L^{\text{m.c.}}(\xi,\eta)=\frac{1-\xi\eta}{2\sqrt{\pi}(1-\xi)^2(1-\eta)^2}\left(\frac{d}{p}\right)^L\frac{(a+2)^{L+3/2}}{L^{3/2}}\times[1+O(L^{-1})]. \tag{3.23}$$

From Eqs. (3.5) and (3.22) one can easily derive that only the L-independent prefactor in Eq. (3.23) changes on the line $\xi=\eta$

$$Z_L^{\text{m.c.}}(\xi,\xi)=\frac{1+\xi}{2\sqrt{\pi}(1-\xi)^3}\left(\frac{d}{p}\right)^L\frac{(a+2)^{L+3/2}}{L^{3/2}}[1+O(L^{-1})]. \tag{3.24}$$

By substituting the above expressions for $Z_L^{\text{m.c.}}(\xi,\eta)$ in Eq. (1.16), we obtain that the large-L asymptotic form of the current in the maximum-current (m.c.) phase is

$$J_L^{\text{m.c.}}=\frac{1-\sqrt{1-p}}{1+\sqrt{1-p}}[1+O(L^{-1})] \tag{3.25}$$

independently of the parameters α and β. In the thermodynamic limit one recovers the well-known mean-field result [9].

B. Current in the low- and high-density phases

At finite L the exact expression for the current in these phases is given by the same ratio of polynomials as in the maximum-current phase, see Eqs. (3.20) and (3.21). Since both the low- and high-density phases take place in regions B, C, and D, the large-L asymptotic form of $Z_L(\xi,\eta)$ for $\xi\neq\eta$ is given, up to exponentially small corrections, by the contribution of the largest eigenvalue of the matrix $C_M(\xi,\eta)$. Since one of the phases maps on the other under the exchange of arguments $\xi\leftrightarrow\eta$, it suffices to consider the case $\xi>\eta$. Appropriate bounds on the correction terms can be obtained by using the inequality $I_L(\xi)\leqslant(a+2)^L I_0(\xi)$, where $I_0(\xi)=1$ for $|\xi|\leqslant 1$ and $I_0(\xi)=\xi^{-2}$ for $|\xi|\geqslant 1$. Thus, for $\xi>1>\eta$ in regions B and C, we obtain from Eq. (3.10) the following bounds on $Z_L^{\text{B,C}}(\xi,\eta)$:

$$\left(\frac{d}{p}\right)^L\frac{\xi-\xi^{-1}}{\xi-\eta}(a+\xi+\xi^{-1})^L\left[1-\frac{\xi\eta}{\xi^2-1}\left(\frac{a+2}{a+\xi+\xi^{-1}}\right)^L\right]$$
$$<Z_L^{\text{B,C}}(\xi,\eta)<\left(\frac{d}{p}\right)^L\frac{\xi-\xi^{-1}}{\xi-\eta}(a+\xi+\xi^{-1})^L\times\left[1+\frac{1}{\xi^2-1}\left(\frac{a+2}{a+\xi+\xi^{-1}}\right)^L\right]. \tag{3.26}$$

In region D, from Eq. (3.14) for $\xi>\eta>1$ and Eq. (3.19) for $\xi=\eta>1$ it follows that the correction terms are also exponentially small in L.

Thus, everywhere in the low-density (l.d.) phase the contribution from the largest eigenvalue dominates over the one from the rest of the spectrum. Hence, up to exponentially small in L corrections

$$J_L^{\text{l.d.}}(\xi,\eta)\simeq(p/d)(a+\xi+\xi^{-1})^{-1}=\frac{\alpha(p-\alpha)}{p(1-\alpha)}. \tag{3.27}$$

The result for the high-density (h.d.) phase follows from Eq. (3.27) under the replacement of ξ by η (i.e., of α by β):

$$J_L^{\text{h.d.}}(\xi,\eta)\simeq(p/d)(a+\eta+\eta^{-1})^{-1}=\frac{\beta(p-\beta)}{p(1-\beta)}. \tag{3.28}$$

Only on the line $\xi=\eta>1$ in region D the current $J_L^{\text{D}}(\xi,\xi)$ has $O(L^{-1})$ corrections to the thermodynamic limit, see Eq. (3.19).

In the thermodynamic limit the above expressions for the current coincide with the corresponding mean-field results [9].

IV. CALCULATION OF THE LOCAL DENSITY

Due to the choice of the matrices D and C, see Eqs. (1.24) and (1.25), respectively, and the vectors $|V\rangle$, $\langle W|$, see Eq. (1.17), the expression for the local density $\rho_L(i)$, $i=1,\ldots,L$, defined in Eq. (1.16), depends only on the elements in the first $[L/2]+1$ rows and columns. Therefore, for the calculation of the scalar product one can use the truncated at $M\geqslant[L/2]+1$ representation of the above-mentioned matrices and vectors,

$$\rho_L(i)=Z_L^{-1}\langle W_M|C_M^{i-1}D_M C_M^{L-i}|V_M\rangle=Z_L^{-1}\langle W_M|U_M\tilde{C}_M^{i-1}\tilde{D}_M\tilde{C}_M^{L-i}U_M^{-1}|V_M\rangle. \tag{4.1}$$

Here $\tilde{C}_M$ is the diagonal form (2.23) of the truncated lattice translation operator C_M, and the transformed truncated matrix $\tilde{D}_M=U_M^{-1}D_M U_M$ has the elements $(m,k=1,\ldots,M)$

$$(\tilde{D}_M)_{m,k}=\frac{d}{p}[Q_L(m,k)+\eta u_M(1,m)u_M(1,k)]+\frac{1-p}{p}\delta_{m,k}, \tag{4.2}$$

where

$$Q_L(m,k)=\sqrt{1-\xi\eta}\,u_M(1,m)u_M(2,k)+\sum_{n=2}^{M-1}u_M(n,m)\times u_M(n+1,k). \tag{4.3}$$

For the sake of simplicity, here we omit the indication of the explicit dependence of the eigenvalues and eigenvectors on the parameters ξ and η, see Eq. (1.20), as well as on the hopping probability p.

By straightforward calculation of the scalar product in Eq. (4.1), we obtain the following general expression for the local density:

$$\rho_L(i)=\frac{d}{pZ_L}[\Omega_L(i)+\eta Z_{i-1}Z_{L-i}+dZ_{L-1}], \tag{4.4}$$

where

$$\Omega_L(i) \equiv \sum_{m=1}^{M} \lambda_M^{i-1}(m) u_M(1,m) \times \sum_{k=1}^{M} \lambda_M^{L-i}(k) u_M(1,k) Q_L(m,k). \quad (4.5)$$

In Sec. III we have found different analytical representations for Z_L in the parameter space shown in Fig. 1. It remains to find the corresponding representations for $\Omega_L(i)$ by using the explicit knowledge of the eigenvalues $\lambda_M(k)$, $k=1,\ldots,M$, and the components of the eigenvectors $u_M(m,n)$, $m,n=1,\ldots,M$, of the matrix C_M. Since their analytical form depends on the values of ξ and η, the derivation is given in Appendix A for region A, and in Appendix B for regions B, C, and D.

A. Local density in the maximum-current phase

This phase appears in region A after taking first the limit $M\to\infty$ and then the limit $L\to\infty$. For finite L and M the eigenvalues of the matrix C_M are given by Eq. (2.17), and the components of the eigenvectors by Eqs. (2.18) and (2.22). After somewhat lengthy transformations, the sums in the right-hand side of Eq. (4.5) can be cast in a form convenient for taking the limit $M\to\infty$. As it is shown in Appendix A, the final exact result for the particle density in the maximum-current phase is

$$\rho_L(i) = \frac{1}{2}(1-J_L^{\mathrm{A}}) + \frac{d}{2pZ_L^{\mathrm{A}}}[F_L(i) - (\xi-\eta) Z_{i-1}^{\mathrm{A}} Z_{L-i}^{\mathrm{A}}]. \quad (4.6)$$

Here $Z_n(\xi,\eta)$ is defined in Eq. (3.3) for $\xi\neq\eta$ and Eq. (3.5) for $\xi=\eta$; $J_L(\xi,\eta)$ is the current in that phase, see Eq. (3.20) for $\xi\neq\eta$ and Eq. (3.21) for $\xi=\eta$; the term $F_L(i;\xi,\eta)$ is an antisymmetric (with respect to the center of the chain) function of the integer coordinate i,

$$F_L(i;\xi,\eta) = -F_L(L-i+1;\xi,\eta), \quad (4.7)$$

defined for $1\leqslant i\leqslant [L/2]$ by the equation

$$F_L(i;\xi,\eta) = \left(\frac{d}{p}\right)^{L-1} (1-\xi\eta) \sum_{n=0}^{L-2i} I_{L-i-n-1}(\xi) I_{i+n-1}(\eta). \quad (4.8)$$

To obtain the particle density profile on the *macroscopic scale* $r=i/L$, as $L\to\infty$, we assume that the lattice site i is far from the two ends of the chain, i.e., $i\gg 1$ and $L-i\gg 1$. Then, for the calculation of $\rho_L(i;\xi,\eta)$ one can use the asymptotic form (3.23) of $Z_n(\xi,\eta)$ for $\xi\neq\eta$, and (3.24) for $\xi=\eta$. Thus, by taking into account the asymptotic form of the current (3.25), we obtain that the position-independent term in the right-hand side of Eq. (4.6) yields the contribution

$$\frac{1}{2}[1-J_L^{\mathrm{m.c.}}(\xi,\eta)] = \frac{\sqrt{1-p}}{1+\sqrt{1-p}}[1+O(L^{-1})]. \quad (4.9)$$

For the contribution of the asymmetric function $F_L(i)$ we obtain as $L\to\infty$

$$\frac{d}{2p}\frac{F_L(i)}{Z_L^{\mathrm{A}}} \simeq \frac{L^{3/2}\sqrt{d}}{4\sqrt{\pi}(1+d)} \sum_{k=0}^{L-2i} \frac{1}{(L-i-k-1)^{3/2}(i+k-1)^{3/2}} \simeq \frac{L^{-1/2}\sqrt{d}}{4\sqrt{\pi}(1+d)} \int_0^{1-2r} \frac{dx}{(1-r-x)^{3/2}(r+x)^{3/2}} = \frac{L^{-1/2}\sqrt{d}}{\sqrt{\pi}(1+d)} \frac{1-2r}{\sqrt{r(1-r)}}. \quad (4.10)$$

The last position-dependent term in Eq. (4.6) yields higher-order corrections $O(L^{-3/2})$.

From the above results it follows that within corrections of order $O(L^{-1/2})$, the density profile $(0<r<1)$

$$\rho_L^{\mathrm{m.c.}}(rL) \simeq \frac{\sqrt{1-p}}{1+\sqrt{1-p}} + \frac{L^{-1/2}\sqrt{d}(1-2r)}{\sqrt{\pi}(1+d)\sqrt{r(1-r)}} \quad (4.11)$$

is independent of the parameters α and β and has the same shape as in the case of stochastic-sequential dynamics, see Eq. (53) in [10]. The above asymptotic form is compared with results of computer simulations in Fig. 4. In the thermodynamic limit $L\to\infty$ the particle density equals exactly the mean-field result for the maximum-current phase.

B. Local density in the low-density phase

The low-density phase exists in regions B, C, and D at $\xi>\eta$, where the contribution from the eigenvector with the single largest eigenvalue (2.44) dominates in the general expression (4.4) for the local density.

The evaluation of $\Omega_L(i)$ in the limit $M\to\infty$ is given in Appendix B. By inserting Eq. (B13) into the general expression (4.4), we obtain the exact result for the local density in the low-density phase in regions B and C at $\xi>\eta$:

$$\rho_L^{\mathrm{B,C}}(i) = \frac{d}{pZ_L^{\mathrm{B,C}}}\left[\frac{\xi-\xi^{-1}}{\xi-\eta}(d+\xi^{-1})\lambda_\infty^{L-1}(1) - (\xi-\xi^{-1}) \times \lambda_\infty^{i-1}(1) Z_{L-i}^{\mathrm{A}} - \frac{\xi-\eta}{2} Z_{L-i}^{\mathrm{A}} Z_{i-1}^{\mathrm{A}} + \frac{p}{2d} Z_L^{\mathrm{A}} - \frac{p}{2d} Z_{L-1}^{\mathrm{A}} + \frac{1}{2} F_L(i)\right]. \quad (4.12)$$

As expected, the asymptotic form of the local density profile at large L differs from the one in the maximum-current phase. The first term in the right-hand side of Eq. (4.12) yields, up to exponentially small in L corrections, the bulk density

$$\frac{d+\xi^{-1}}{a+\xi+\xi^{-1}} = \frac{\alpha(1-p)}{p(1-\alpha)}. \quad (4.13)$$

The leading-order contribution of the second term

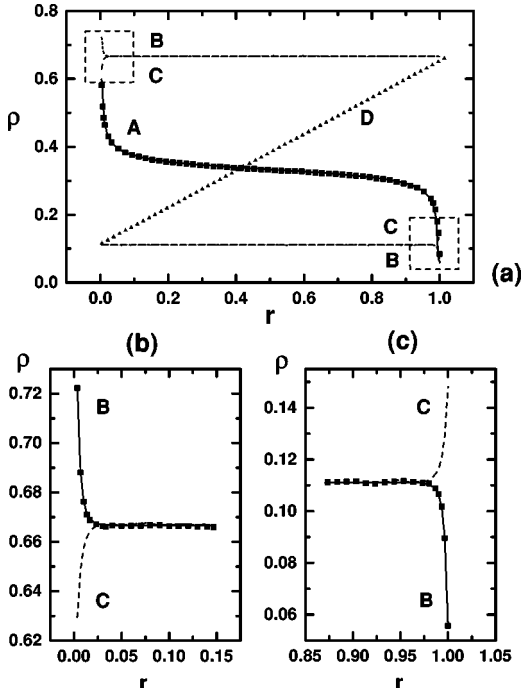

FIG. 4. Particle density profiles versus the scaled distance $r=i/L$ in the different regions of Fig. 1. The results of computer simulations for a chain of length $L=300$ are shown in part (a) by solid squares (region A), solid triangles (on the coexistence line in region D), and dashed lines (regions B and C); all lines are labeled by the letter of the corresponding region. The solid line shows the asymptotic behavior described by Eq. (4.10) in region A. Parts (b) and (c) of the figure show the enlarged portions of part (a) enclosed in dashed squares close to the left and right ends of the chain, respectively. The asymptotic behavior described by Eq. (4.16) in the low-density phase and Eq. (4.27) in the high-density phase is shown by solid lines in region B and dashed lines in region C; the results of computer simulations in region B are shown by solid squares.

$$-\frac{\xi I_{L-i}(\xi)-\eta I_{L-i}(\eta)}{(a+\xi+\xi^{-1})^{L-i+1}} \tag{4.14}$$

is exponentially small in L, except close to the right boundary.

All the remaining terms are uniformly in $i=1,\ldots,L$ bounded from above by an exponentially small in L quantity of the order

$$\left(\frac{a+2}{a+\xi+\xi^{-1}}\right)^{L}, \quad \xi\neq 1. \tag{4.15}$$

By collecting the above results we obtain that up to exponentially small in L corrections the local density of the low-density phase in regions B and C is given by

$$\rho_L^{\mathrm{B,C}}(i)\simeq\frac{\alpha(1-p)}{p(1-\alpha)}-\frac{\xi I_{L-i}(\xi)-\eta I_{L-i}(\eta)}{(a+\xi+\xi^{-1})^{L-i+1}}. \tag{4.16}$$

The qualitatively different behavior of the particle density profile in the maximum-current and low-density phases is illustrated by results of computer simulations in Fig. 4. One clearly sees that even for a rather small system the shape of $\rho_L(rL;\xi,\eta)$ as a function of the scaled distance $r=i/L$ drastically changes on crossing the phase boundary. In the maximum-current phase the profile has power-law deviations from the bulk value, which are of opposite sign near the left and right ends of the chain, and vanish as $O(L^{-1/2})$ when $L\to\infty$. In the low-density phase, the profile is constant (up to exponentially small in L terms) near the left end of the chain, and changes exponentially fast with the distance near the right end. To analyze the sign of that exponential change, we note that, as follows from Eq. (3.5),

$$\frac{\partial}{\partial\xi}[\xi I_n(\xi)]=(1-\xi^2)K_n(\xi) \tag{4.17}$$

changes sign at $\xi=1$. Since in the low-density phase $\xi>1>\eta$, we use the relationship (3.11) to write

$$\xi I_{L-i}(\xi)-\eta I_{L-i}(\eta)=\xi^{-1}I_{L-i}(\xi^{-1})-\eta I_{L-i}(\eta).$$

Obviously, this expression is positive in region B ($\xi^{-1}>\eta$), and negative in region C ($\xi^{-1}<\eta$). Therefore, the bending of the profile near the right end of the chain is downward in region B and upward in region C.

The exponential approach to the bulk density as $L-i\to\infty$, predicted by the position-dependent term in Eq. (4.16), is in exellent agreement with the results of computer simulations; see Fig. 4. Note that the bulk density coincides with the known mean-field result [9]. The asymptotic form (4.16) can be checked against the exact relationships between the current and the local density at the end-points of the chain. Such relationships follow directly from the general expressions (1.16) for J_L and $\rho_L(i)$ and the boundary conditions (1.15), see, e.g., [9]. Thus, by setting $i=1$ and using the left boundary condition one obtains

$$\rho_L(1;\xi,\eta)=1-\alpha^{-1}J_L(\xi,\eta). \tag{4.18}$$

On the other hand, by setting $i=L$ and using the right boundary condition one finds

$$\rho_L(L;\xi,\eta)=(\beta^{-1}-1)J_L(\xi,\eta). \tag{4.19}$$

By substituting the asymptotic form (3.27) of the current in Eq. (4.18) one obtains (up to exponentially small in L corrections) that $\rho_L^{\mathrm{l.d.}}(1)=\rho_{bulk}^{\mathrm{l.d.}}$. In a similar way, from Eq. (4.19) one has

$$\rho_L^{\mathrm{l.d.}}(L)=\frac{\alpha(1-\beta)(p-\alpha)}{\beta p(1-\alpha)}. \tag{4.20}$$

The above result coincides with the right-hand side of Eq. (4.16) at $i=L$.

In region D we obtain from Eqs. (4.4) and (B17) the following exact expression for the local density ($\xi\neq\eta$):

$$\rho_L^{\rm D}(i)=\frac{1-p}{p}J_L^{\rm D}(\xi,\eta)+\frac{d}{pZ_L^{\rm D}}\Bigg[\frac{1-\xi^{-2}}{\xi-\eta}\lambda_\infty^{L-1}(1)+\frac{(\xi-\xi^{-1})(\eta-\eta^{-1})}{\xi-\eta}\lambda_\infty^{i-1}(1)\lambda_\infty^{L-i}(2)-\frac{\eta^2-1}{\xi-\eta}\lambda_\infty^{L-1}(2)\Bigg]+\frac{d}{pZ_L^{\rm D}}[-(\xi-\xi^{-1})\lambda_\infty^{i-1}(1)Z_{L-i}^{\rm A}+(\eta-\eta^{-1})\lambda_\infty^{L-i}(2)Z_{i-1}^{\rm A}+\eta Z_{i-1}^{\rm A}Z_{L-i}^{\rm A}+\Omega_L^{\rm A}(i)]. \tag{4.21}$$

The part of region D occupied by the low-density phase corresponds to $\xi>\eta>1$. Hence, by taking into account Eq. (3.14) for $Z_L^{\rm D}$ and Eq. (3.27) for the current, after neglecting terms which are uniformly in $i=1,\ldots,L$ exponentially small as $L\to\infty$, we obtain that the local density in region D is

$$\rho_L^{\rm D}(i)\simeq\frac{\alpha(1-p)}{p(1-\alpha)}+\frac{\eta-\eta^{-1}}{a+\xi+\xi^{-1}}\left(\frac{a+\eta+\eta^{-1}}{a+\xi+\xi^{-1}}\right)^{L-i}-\frac{\xi I_{L-i}(\xi)-\eta I_{L-i}(\eta)}{(a+\xi+\xi^{-1})^{L-i+1}}. \tag{4.22}$$

A comparison with Eq. (4.16) reveals an important new feature: the leading-order analytic form of the density profile changes on passing from region C to region D *within* the low-density phase. Nevertheless, the density profile has a similar shape in regions C and D, since it is constant (up to exponentially small in L corrections) near the left end of the chain, and tends to the bulk value exponentially fast (although with different rate) as the distance from the right end increases; the bending of the density profile near the right end of the chain is upward in both regions C and D. One can readily check that at $i=L$ the local density (4.22) also satisfies the boundary condition (4.20).

C. Local density in the high-density phase

The high-density phase exists in regions B, C, and D at $\eta>\xi$. The expression for $\Omega_L(i)$ follows by exchanging places of ξ and η in Eq. (B13) [note that $Z_L^{\rm A}(\xi,\eta)$ is a symmetric polynomial in ξ and η]. By inserting the result in the general Eq. (4.4), we obtain the exact expression for the local density in the high-density phase in regions B and C at $\eta>\xi$:

$$\rho_L^{\rm B,C}(i)=\frac{d}{pZ_L^{\rm B,C}}\Bigg[\frac{\eta-\eta^{-1}}{\eta-\xi}(d+\eta)\lambda_\infty^{L-1}(1)+(\eta-\eta^{-1})\times\lambda_\infty^{L-i}(1)Z_{i-1}^{\rm A}+\frac{\eta-\xi}{2}Z_{i-1}^{\rm A}Z_{L-i}^{\rm A}+\frac{p}{2d}Z_L^{\rm A}-\frac{p}{2d}Z_{L-1}^{\rm A}+\frac{1}{2}F_L(i)\Bigg]. \tag{4.23}$$

The symmetry transformation $\xi\leftrightarrow\eta$ and $i\leftrightarrow L-i+1$ brings *all the position-dependent terms* in the local density (4.23) to the form of the corresponding terms in the low-density phase, see Eq. (4.12), taken with the *opposite sign*. Note that $F_L(i;\xi,\eta)$, see Eqs. (4.7) and (4.8), is a symmetric function of ξ and η, but changes sign under the coordinate transformation $i\leftrightarrow L-i+1$. This fact explains the antisymmetry in the bending of the density profiles in the two phases at the opposite ends of the chain, see also the computer simulation results shown in Fig. 4.

By ignoring the exponentially small as $L\to\infty$ corrections, one obtains that the first term in the right-hand side of Eq. (4.12) yields the bulk density

$$\frac{d+\eta}{a+\eta+\eta^{-1}}=1-\frac{\beta}{p}. \tag{4.24}$$

The leading-order contribution of the second term

$$\frac{\eta I_{i-1}(\eta)-\xi I_{i-1}(\xi)}{(a+\eta+\eta^{-1})^i} \tag{4.25}$$

is exponentially small in L, except close to the left boundary.

All the remaining terms are uniformly in $i=1,\ldots,L$ bounded from above by an exponentially small quantity of the order

$$\left(\frac{a+2}{a+\eta+\eta^{-1}}\right)^L,\quad \eta\neq 1. \tag{4.26}$$

By collecting the above results we obtain that up to exponentially small in L corrections the local density of the high-density phase in regions B and C is

$$\rho_L^{\rm B,C}(i)\simeq 1-\frac{\beta}{p}+\frac{\eta I_{i-1}(\eta)-\xi I_{i-1}(\xi)}{(a+\eta+\eta^{-1})^i}. \tag{4.27}$$

Thus, in the high-density phase the profile is constant (up to exponentially small in L terms) near the right end of the chain, and changes exponentially fast with the distance near the left end. The profile bends upward in region B and downward in region C. This behavior is in excellent agreement with the results of computer simulations; see Fig. 4. Note that the bulk density (4.24) coincides with the known mean-field result [9].

The asymptotic form (4.27) agrees (up to exponentially small in L corrections) with the exact relationships between the current and the local density at the end-points of the chain, see Eqs. (4.18) and (4.19). Indeed, from Eqs. (3.28) and (4.18) one obtains at the left end of the chain

$$\rho_L^{\rm h.d.}(1)=1-\frac{\beta(p-\beta)}{\alpha p(1-\beta)}, \tag{4.28}$$

which coincides with Eq. (4.27) at $i=1$. At the right end $\rho_L^{\rm h.d.}(L)=\rho_{bulk}^{\rm h.d.}$.

The asymptotic form of the density profile in the high-density phase occupying region D, i.e., when $\eta>\xi>1$, follows directly from the exact expressions (4.21) for $\rho_L^{\rm D}(i)$ and (3.14) for $Z_L^{\rm D}$, after neglecting terms which are uniformly in $i=1,\ldots,L$ exponentially small as $L\to\infty$:

$$\rho_L^{\mathrm{D}}(i)\simeq 1-\frac{\beta}{p}-\frac{\xi-\xi^{-1}}{a+\eta+\eta^{-1}}\left(\frac{a+\xi+\xi^{-1}}{a+\eta+\eta^{-1}}\right)^{i-1}+\frac{\eta I_{i-1}(\eta)-\xi I_{i-1}(\xi)}{(a+\eta+\eta^{-1})^{i}}. \tag{4.29}$$

As in region C, the profile bends downward near the left end of the chain and satisfies the boundary condition (4.28) at $i=1$. Similarly to the case of the low-density phase, the leading-order asymptotic form of the position-dependent terms changes on passing from region C to region D *within* the high-density phase; compare Eqs. (4.27) and (4.29).

D. Local density on the coexistence line

The condition $\xi=\eta>1$ defines the coexistence line between the low- and high-density phases in region D. By inserting Eq. (B19) for $\Omega_L^{\mathrm{D}}(i;\xi,\xi)$ into the general expression (4.4) for the local density, we obtain the exact result

$$\begin{aligned}\rho_L^{\mathrm{coex}}(i;\xi,\xi)=\frac{d}{pZ_L^{\mathrm{D}}(\xi,\xi)}\Big\{&(\xi-\xi^{-1})[\lambda_\infty^{L-i}(1)Z_{i-1}^{\mathrm{A}}(\xi,\xi)\\&-\lambda_\infty^{i-1}(1)Z_{L-i}^{\mathrm{A}}(\xi,\xi)]+(\xi+\xi^{-3})\lambda_\infty^{L-1}(1)\\&-(\xi-\xi^{-1})^2\frac{d}{p}\lambda_\infty^{L-2}(1)+(1-\xi^{-2})^2\\&\times[L+(\xi^2-1)i]\frac{d}{p}\lambda_\infty^{L-2}(1)\\&+\xi Z_{i-1}^{\mathrm{A}}(\xi,\xi)Z_{L-i}^{\mathrm{A}}(\xi,\xi)+\Omega_L^{\mathrm{A}}(i;\xi,\xi)\Big\}\\&+\frac{1-p}{p}J_L^{\mathrm{D}}(\xi,\xi).\end{aligned} \tag{4.30}$$

By assuming *macroscopic scale* of distance, i.e., considering $i/L=O(1)$ as $L\to\infty$, and by ignoring the $O(L^{-1})$ corrections we obtain the linear density profile

$$\rho_L^{\mathrm{coex}}(rL;\xi,\xi)\simeq\frac{1}{a+\xi+\xi^{-1}}[d+\xi^{-1}+(\xi-\xi^{-1})r]. \tag{4.31}$$

It is readily seen that, up to $O(L^{-1})$ corrections, the local density on the coexistence line changes linearly from the bulk density of the low-density phase at the left end of the chain ($r=0$), to the bulk density of the high-density phase at the right end ($r=1$); see Fig. 4.

V. DISCUSSION

For the FASEP with open boundary conditions we have calculated exactly the current and the local particle density, both for finite chains and in the thermodynamic limit. It should be emphasized that our results are not based on a finite-dimensional representation of the relevant algebra given by Eqs. (1.14) and (1.15). The truncated matrices D_M and E_M *do not* solve the bulk algebra (1.14) because of a defect in the last element on the main diagonal of the product matrix D_ME_M. Firstly, we find an infinite-dimensional representation for the operators D and E, such that the lattice translation operator $C=E+D$ is (real or complex) symmetric. Secondly, we exploit the fact that for a finite chain of size L the quantities of interest depend only on the elements in the first $[L/2]+1$ rows and columns of C and D. This makes possible the use of truncated M-dimensional matrices, with $M\geqslant[L/2]+1$, for the calculation of the finite-size current, J_L, and density profile, $\rho_L(i)$, $i=1,\ldots,L$. Thirdly, we perform the calculations after diagonalization of the truncated propagator C_M by means of similarity transformation with a symmetric (real or complex) matrix. At this step the spectrum of C_M reveals the crucial role of the parameters ξ and η in the mathematical mechanism of the phase transition: if at least one of ξ and η exceeds unity, the largest eigenvalue singles out from the bounded quasicontinuous spectrum and its contribution becomes dominant at large L. Fourthly, we lift the truncation by passing to the limit $M\to\infty$. In this limit the expressions obtained simplify essentially and become valid for all L. The resulting integral representations clearly show that for any finite L the current and the local particle density are real analytical functions of the parameters. Only in the thermodynamic limit $L\to\infty$ do these quantities develop different analytical forms in the maximum-current, low-density, and high-density phases. When both α and β are less than $1-\sqrt{1-p}$, two large eigenvalues appear. This causes a change of the leading-order asymptotic form of the position-dependent part of the local density within a single phase. The two largest eigenvalues become degenerate on the coexistence line $\alpha=\beta$ between the low- and high-density phases, which manifests itself in the appearance of a linear profile of the local density.

The exact expressions for the bulk current and bulk density are found to coincide with the analytic continuation of the corresponding mean-field results from the line $(1-\alpha)(1-\beta)=1-p$ to the entire parameter space. This has been conjectured in [9] on the basis of computer simulations. On the grounds that the above line *touches* all phases, and that the analytic form of the current and bulk density does not change within a phase, the validity of the corresponding expressions for the whole phases has been conjectured [9]. However, these arguments do not have the status of a proof, especially for the maximum-current phase which is touched by the mean-field line just at one corner point of the phase boundary. In our work, in addition to the above-mentioned bulk quantities, we have calculated exactly the density profiles in all the phases. We have shown that the asymptotic form of the profile changes when α or β crosses the value $1-\sqrt{1-p}$ in the high- or low-density phases, respectively. A similar fact has been established in the case of random-sequential dynamics [11]. To our knowledge, the results for the density profiles found here for the ordered-sequential dynamics are new.

APPENDIX A

Here we derive an exact expression for the site-dependent quantity $\Omega_L(i)$, $i=1,\ldots,L$, defined in Eq. (4.5), by taking the limit $M\to\infty$ in the maximum-current phase, region A. First we perform the summation in Eq. (4.3) for $Q_L(m,k)$ and after some transformations cast the result in the form

$$Q_L(m,k)=Q_L^{(s)}(m,k)+Q_L^{(a)}(m,k). \tag{A1}$$

Here $Q_L^{(s)}(m,k)$ is the symmetric (with respect to m and k) part of $Q_L(m,k)$, the explicit expression for which depends on whether $m\neq k$ or $m=k$. For $m\neq k$

$$\begin{aligned}Q_L^{(s)}(m,k)&=-\frac{1}{2}\frac{\xi+\eta}{1-\xi\eta}b_M(m)b_M(k)\\&\quad\times\sin[M\phi_M(m)]\sin[M\phi_M(k)]\\&=-\frac{1}{2}(\xi+\eta)u_M(1,m)u_M(1,k).\end{aligned} \tag{A2}$$

In deriving the second equality we have used Eq. (2.18). For $m=k$ we obtain

$$\begin{aligned}Q_L^{(s)}(k,k)&=\frac{1}{2}b_M^2(k)\left[M\cos\phi_M(k)-\frac{\sin[2M\phi_M(k)]}{2\sin\phi_M(k)}\right]\\&=\frac{1}{2}b_M^2(k)\left[M\cos\phi_M(k)\right.\\&\quad\left.-\frac{(1-\xi\eta)[\xi+\eta-(1+\xi\eta)\cos\phi_M(k)]}{R_M(k;\xi)R_M(k;\eta)}\right],\end{aligned} \tag{A3}$$

where

$$R_M(k;\xi)=1-2\xi\cos\phi_M(k)+\xi^2. \tag{A4}$$

The antisymmetric (with respect to the exchange of m and k) part of $Q_L(m,k)$ is defined for $m\neq k$ by

$$\begin{aligned}Q_L^{(a)}(m,k)&=\frac{1}{2}b_M(m)b_M(k)\frac{\sin\phi_M(m)\sin\phi_M(k)}{\cos\phi_M(m)-\cos\phi_M(k)}\\&\quad-\frac{R_M(m;\xi)R_M(k;\eta)+R_M(m;\eta)R_M(k;\xi)}{4(1-\xi\eta)}\\&\quad\times\frac{u_M(1,m)u_M(1,k)}{\cos\phi_M(m)-\cos\phi_M(k)}.\end{aligned} \tag{A5}$$

In the limit $M\to\infty$ the contribution of the term (A2) into $\Omega_L(i)$ is

$$-\frac{1}{2}(\xi+\eta)Z_{i-1}^{\mathrm{A}}Z_{L-i}^{\mathrm{A}}. \tag{A6}$$

The term (A3) appears in the single sum ($m=k$)

$$\sum_{k=1}^{M}\lambda_M^{L-1}(k)u_M^2(1,k)Q_L^{(s)}(k,k), \tag{A7}$$

and only the part of $Q_L^{(s)}(k,k)$ which is proportional to $M\cos\phi_M(k)$ yields the nonvanishing in the limit $M\to\infty$ contribution

$$\begin{aligned}&\left(\frac{d}{p}\right)^{L-1}\frac{2}{\pi}\int_0^{\pi}\mathrm{d}\phi\,\frac{(a+2\cos\phi)^{L-1}\sin^2\phi\cos\phi}{1+\xi^2-2\xi\cos\phi}\\&\quad=\frac{1}{2}\left[\frac{p}{d}Z_L^{\mathrm{A}}(\xi,\eta)-aZ_{L-1}^{\mathrm{A}}(\xi,\eta)\right].\end{aligned} \tag{A8}$$

Consider now the contribution of the antisymmetric term (A5) into $\Omega_L(i)$. By using the antisymmetry of $Q_L^{(a)}(m,k)$ with respect to m and k, we write

$$\begin{aligned}\Omega_L^{(a)}(i)&=\frac{1}{2}\sum_{m=1}^{M}\sum_{k=1}^{M}{}'\,[\lambda_M^{i-1}(m)\lambda_M^{L-i}(k)\\&\quad-\lambda_M^{i-1}(k)\lambda_M^{L-i}(m)]u_M(1,m)u_M(1,k)Q_L^{(a)}(m,k).\end{aligned} \tag{A9}$$

The primed summation means that the term with $m=k$ is excluded from the double sum. As one can readily see, $\Omega_L^{(a)}(i)$ changes sign under the coordinate transformation $i\to L-i+1$; if $L+1$ is even then $\Omega_L^{(a)}(i)$ vanishes at the center of the lattice, $i=[(L+1)/2]$. To take the limit $M\to\infty$ we assume $2i<L+1$ and write

$$\begin{aligned}\Omega_L^{(a)}(i)&=-\frac{d}{p}\sum_{n=0}^{L-2i}\sum_{m=1}^{M}\sum_{k=1}^{M}{}'\,\lambda_M^{L-i-n-1}(m)\lambda_M^{i+n-1}(k)\\&\quad\times u_M(1,m)u_M(1,k)[\cos\phi_M(m)\\&\quad-\cos\phi_M(k)]Q_L^{(a)}(m,k).\end{aligned} \tag{A10}$$

Now the first term in the right-hand side of Eq. (A5) yields

$$\begin{aligned}&-\frac{1-\xi\eta}{2}\frac{d}{p}\sum_{n=0}^{L-2i}\sum_{m=1}^{M}\sum_{k=1}^{M}{}'\,\lambda_M^{L-i-n-1}(m)\lambda_M^{i+n-1}(k)\\&\quad\times(-1)^{m+k}\frac{b_M^2(m)\sin^2\phi_M(m)}{\sqrt{R_M(m;\xi)R_M(m;\eta)}}\\&\quad\times\frac{b_M^2(k)\sin^2\phi_M(k)}{\sqrt{R_M(k;\xi)R_M(k;\eta)}}.\end{aligned} \tag{A11}$$

Due to the factor $(-1)^{m+k}$ in the summand, this part of $\Omega_L^{(a)}(i)$ vanishes as $M\to\infty$ since the leading asymptotic forms for $m+k$ even and odd integer cancel. For $2i<L+1$, the contribution of the second term in the right-hand side of Eq. (A5) in the limit $M\to\infty$ is

$$\frac{1-\xi\eta}{2}\left(\frac{d}{p}\right)^{L-1}\sum_{n=0}^{L-2i}I_{L-i-n-1}(\xi)I_{i+n-1}(\eta)\equiv\frac{1}{2}F_L(i;\xi,\eta). \tag{A12}$$

By collecting the above results one obtains in region A

$$\Omega_L^{\mathrm{A}}(i)=\frac{1}{2}\left[F_L(i)-(\xi+\eta)Z_{i-1}^{\mathrm{A}}Z_{L-i}^{\mathrm{A}}+\frac{p}{d}Z_L^{\mathrm{A}}-aZ_{L-1}^{\mathrm{A}}\right]. \tag{A13}$$

Finally, by inserting this result into Eq. (4.4), one obtains expression (4.6) for the local particle density in the maximum current phase.

APPENDIX B

Here we evaluate $\Omega_L(i)$ in regions B, C, and D. First we consider explicitly region B; the results for region C have the same analytical form. Then, in region D we take into account the contribution of the next-to-the-largest eigenvalue $\lambda_M(2)$, see below.

By singling out the contributions of the eigenvector with the largest eigenvalue, we write

$$\Omega_L(i)=\lambda_M^{L-1}(1)u_M^2(1,1)Q_L(1,1)+\lambda_M^{i-1}(1)u_M(1,1)\sum_{k=2}^{M}\lambda_M^{L-i}(k)u_M(1,k)Q_L(1,k)+\lambda_M^{L-i}(1)u_M(1,1)\sum_{m=2}^{M}\lambda_M^{i-1}(m)u_M(1,m)Q_L(m,1)+\Omega_L'(i). \tag{B1}$$

In region B we have the explicit expressions

$$Q_L(1,1)=b_M^2(1)\sum_{n=1}^{M-1}\sinh[(M+1-n)\phi_M(1)]\times\sinh[(M-n)\phi_M(1)],$$

$$Q_L(1,k)=b_M(1)b_M(k)\sum_{n=1}^{M-1}\sinh[(M+1n)\phi_M(1)]\times\sin[(M-n)\phi_M(k)], \tag{B2}$$

$$Q_L(m,1)=b_M(1)b_M(m)\sum_{n=1}^{M-1}\sin[(M+1-n)\phi_M(m)]\times\sinh[(M-n)\phi_M(1)].$$

The last term in the right-hand side of Eq. (B1), namely $\Omega_L'(i)$, differs from $\Omega_L(i)$ defined in Eq. (4.5) only in that the sums over m and k run from 2 to M. Therefore, in the limit $M\to\infty$ this term yields in regions B and C the same result as in region A, see Eq. (A13),

$$\lim_{M\to\infty}\Omega_L'(i)=\Omega_L^{\mathrm{A}}(i). \tag{B3}$$

By direct evaluation of the sums in Eqs. (B2) we obtain

$$Q_L(1,1)=\frac{1}{2}b_M^2(1)\left[\frac{\sinh[2M\phi_M(1)]}{2\sinh\phi_M(1)}-M\cosh\phi_M(1)\right], \tag{B4}$$

$$Q_L^{(s)}(1,k)\equiv\frac{1}{2}[Q_L(1,k)+Q_L(k,1)]=-\frac{1}{2}(\xi+\eta)u_M(1,1)u_M(1,k), \tag{B5}$$

$$Q_L^{(a)}(1,k)\equiv\frac{1}{2}[Q_L(1,k)-Q_L(k,1)]=\frac{b_M(1)b_M(k)\sinh\phi_M(1)\sin\phi_M(k)}{2[\cosh\phi_M(1)-\cos\phi_M(k)]}-\frac{\tilde{R}_M(1;\xi)R_M(k;\eta)+\tilde{R}_M(1;\eta)R_M(k;\xi)}{4(1-\xi\eta)}\times\frac{u_M(1,1)u_M(1,k)}{[\cosh\phi_M(1)-\cos\phi_M(k)]}, \tag{B6}$$

where

$$\tilde{R}_M(1;\xi)=1-2\xi\cosh\phi_M(1)+\xi^2. \tag{B7}$$

With the aid of the limits (3.8) and

$$\lim_{M\to\infty}\phi_M(1)=\ln\xi,\quad\lim_{M\to\infty}Q_L(1,1)=\frac{1-\xi\eta}{\xi-\eta}\quad(\xi>\eta), \tag{B8}$$

we evaluate the contribution of the first term in the right-hand side of Eq. (B1) for $\xi>\eta$

$$\frac{(\xi-\xi^{-1})(1-\xi\eta)}{(\xi-\eta)^2}\lambda_\infty^{L-1}(1). \tag{B9}$$

By using Eqs. (B5) and (B6) we reorganize the contributions of the second and third terms in the right-hand side of Eq. (B1) into symmetric and antisymmetric parts. The straightforward evaluation of the symmetric part yields in the limit $M\to\infty$ $(\xi>\eta)$

$$-\frac{1}{2}(\xi+\eta)\frac{\xi-\xi^{-1}}{\xi-\eta}[\lambda_\infty^{i-1}(1)Z_{L-i}^{\mathrm{A}}+\lambda_\infty^{L-i}(1)Z_{i-1}^{\mathrm{A}}]. \tag{B10}$$

Turning to the antisymmetric part, we first notice that the contribution of the first term in the right-hand side of Eq. (B6) vanishes in the limit $M\to\infty$. The contribution of the second term is easily obtained with the aid of the limits

$$\lim_{M\to\infty}\tilde{R}_M(1;\xi)=0,\qquad\lim_{M\to\infty}\tilde{R}_M(1;\eta)=\xi^{-1}(1-\xi\eta)(\xi-\eta)\quad(\xi>\eta). \tag{B11}$$

As a result, the antisymmetric part yields

$$-\frac{1}{2}(\xi-\xi^{-1})[\lambda_\infty^{i-1}(1)Z_{L-i}^{\mathrm{A}}-\lambda_\infty^{L-i}(1)Z_{i-1}^{\mathrm{A}}]. \tag{B12}$$

By collecting the above terms we obtain for $\xi>\eta$

$$\Omega_L^{\mathrm{B,C}}(i)=\frac{\xi-\xi^{-1}}{\xi-\eta}\left[\frac{1-\xi\eta}{\xi-\eta}\lambda_\infty^{L-1}(1)-\xi\lambda_\infty^{i-1}(1)Z_{L-i}^{\mathrm{A}}-\eta\lambda_\infty^{L-i}(1)Z_{i-1}^{\mathrm{A}}\right]+\Omega_L^{\mathrm{A}}(i). \tag{B13}$$

The result for $\eta>\xi$ follows by exchanging places of ξ and η.

In region D we single out the contributions of the eigenvectors $|u_M(1)\rangle$ and $|u_M(2)\rangle$ in the general expression (4.5) for $\Omega_L(i)$. The evaluation of the kernel $Q_L(m,k)$, see Eq. (4.3), is performed by using the explicit form of the eigenvectors in region D. For the part of $\Omega_L(i)$ which involves only the eigenvectors with eigenvalues $\lambda_M(1)$ and/or $\lambda_M(2)$ we obtain

$$
\begin{aligned}
&-\lambda_M^{L-1}(1)u_M^2(1,1)Q_L(1,1)+\lambda_M^{L-1}(2)u_M^2(1,2)Q_L(2,2)\\
&\quad+[\lambda_M^{i-1}(1)\lambda_M^{L-i}(2)\\
&\quad+\lambda_M^{L-i}(1)\lambda_M^{i-1}(2)]u_M(1,1)u_M(1,2)Q_L^{(s)}(1,2)\\
&\quad+[\lambda_M^{i-1}(1)\lambda_M^{L-i}(2)\\
&\quad-\lambda_M^{L-i}(1)\lambda_M^{i-1}(2)]u_M(1,1)u_M(1,2)Q_L^{(a)}(1,2). \qquad \text{(B14)}
\end{aligned}
$$

Here $Q_L(1,1)$ is defined by the first equation (B2), and $Q_L(2,2)$ follows from the latter by replacing $\phi_M(1)$ with $\phi_M(2)$; $Q_L^{(s)}(1,2)$ and $Q_L^{(a)}(1,2)$ are the symmetric and antisymmetric (with respect to the labels 1 and 2) parts of

$$
\begin{aligned}
Q_L(1,2)=&-\mathrm{i}\,b_M(1)b_M(2)\sum_{n=1}^{M-1}\sinh[(M+1-n)\phi_M(1)]\\
&\times\sinh[(M-n)\phi_M(2)].
\end{aligned}
$$

The part of $\Omega_L(i)$ which involves one of the two largest eigenvalues and the bounded quasicontinuous spectrum is

$$
\begin{aligned}
&\sum_{j=1}^{2}\sum_{k=3}^{M}[\lambda_M^{i-1}(j)\lambda_M^{L-i}(k)\\
&\quad+\lambda_M^{L-i}(j)\lambda_M^{i-1}(k)]u_M(1,j)u_M(1,k)Q_L^{(s)}(j,k)\\
&\quad+\sum_{j=1}^{2}\sum_{k=3}^{M}[\lambda_M^{i-1}(j)\lambda_M^{L-i}(k)\\
&\quad-\lambda_M^{L-i}(j)\lambda_M^{i-1}(k)]u_M(1,j)u_M(1,k)Q_L^{(a)}(j,k). \qquad \text{(B15)}
\end{aligned}
$$

Here $Q_L^{(s)}(1,k)$ and $Q_L^{(a)}(1,k)$ $(k=3,\ldots,M)$ are defined in Eqs. (B5) and (B6), respectively; $Q_L^{(s)}(2,k)$ and $Q_L^{(a)}(2,k)$ follow under replacement of $\phi_M(1)$ by $\phi_M(2)$. The contribution of these terms in the limit $M\to\infty$ is readily obtained by taking into account the limits (3.8), (3.9), (B11), and

$$
\lim_{M\to\infty}\tilde{R}_M(2;\xi)=\eta^{-1}(\xi\eta-1)(\xi-\eta),\quad \lim_{M\to\infty}\tilde{R}_M(2;\eta)=0. \qquad \text{(B16)}
$$

All the remaining terms in $\Omega_L(i)$ involve only eigenvalues belonging to the quasicontinuous part of the spectrum of the matrix C_M; they yield in the limit $M\to\infty$ the same analytical expression (A13) as the one for $\Omega_L(i)$ in region A (however, with ξ and η larger than unity).

As a result, by taking the limit $M\to\infty$ at $\xi>\eta>1$ we obtain the exact expression

$$
\begin{aligned}
\Omega_L^{\mathrm{D}}(i;\xi,\eta)=&-\frac{\xi\eta-1}{(\xi-\eta)^2}[(\xi-\xi^{-1})\lambda_\infty^{L-1}(1)+(\eta-\eta^{-1})\lambda_\infty^{L-1}(2)]\\
&+\frac{(\xi-\xi^{-1})(\eta-\eta^{-1})}{(\xi-\eta)^2}[\xi\lambda_\infty^{i-1}(1)\lambda_\infty^{L-i}(2)+\eta\lambda_\infty^{L-i}(1)\lambda_\infty^{i-1}(2)]\\
&-\frac{1}{\xi-\eta}[(\xi^2-1)\lambda_\infty^{i-1}(1)-(\eta^2-1)\lambda_\infty^{i-1}(2)]Z_{L-i}^{\mathrm{A}}(\xi,\eta)\\
&-\frac{1}{\xi-\eta}[\eta(\xi-\xi^{-1})\lambda_\infty^{L-i}(1)-\xi(\eta-\eta^{-1})\lambda_\infty^{L-i}(2)]Z_{i-1}^{\mathrm{A}}(\xi,\eta)+\Omega_L^{\mathrm{A}}(i;\xi,\eta). \qquad \text{(B17)}
\end{aligned}
$$

The same result holds also for $\eta>\xi>1$, since the right-hand side of Eq. (B17) is invariant under the transformation $\xi\leftrightarrow\eta$, which implies $\lambda_\infty(1)\leftrightarrow\lambda_\infty(2)$.

Note that the singularity at $\xi=\eta$ in the right-hand side of Eq. (B17) can be removed with the aid of the equality

$$
\lambda_\infty(1)-\lambda_\infty(2)=\frac{d}{p}\,\frac{(\xi-\eta)(\xi\eta-1)}{\xi\eta}.
$$

Thus, by taking into account Eq. (3.14) for $Z_L^{\mathrm{D}}(\xi,\eta)$, we can rewrite Eq. (B17) in the equivalent form

$$
\begin{aligned}
\Omega_L^{\mathrm{D}}(i;\xi,\eta)=&-\eta Z_{i-1}^{\mathrm{D}}(\xi,\eta)Z_{L-i}^{\mathrm{D}}(\xi,\eta)+\left(\xi^{-1}+\eta-\frac{\xi-\xi^{-1}}{\xi\eta}\right)\lambda_\infty^{L-1}(1)+\frac{d}{p}\,\frac{(\eta^2-1)(\xi\eta-1)}{\xi\eta}\\
&\times\left[\sum_{n=0}^{L-2}\lambda_\infty^{L-n-2}(1)\lambda_\infty^{n}(2)-\frac{\xi^2-1}{\xi\eta}\sum_{n=0}^{L-i-1}\lambda_\infty^{L-n-2}(1)\lambda_\infty^{n}(2)\right]\\
&-(\xi-\xi^{-1})\lambda_\infty^{i-1}(1)Z_{L-i}^{\mathrm{A}}(\xi,\eta)+(\eta-\eta^{-1})\lambda_\infty^{L-i}(2)Z_{i-1}^{\mathrm{A}}(\xi,\eta)
\end{aligned}
$$

$$+\Omega_L^{\mathrm{A}}(i;\xi,\eta)+\eta Z_{i-1}^{\mathrm{A}}(\xi,\eta)Z_{L-i}^{\mathrm{A}}(\xi,\eta). \tag{B18}$$

The above expression is convenient for the study of the coexistence line $\xi=\eta>1$: by setting $\eta=\xi$ we obtain

$$\Omega_L^{\mathrm{D}}(i;\xi,\xi)=-\xi Z_{i-1}^{\mathrm{D}}(\xi,\xi)Z_{L-i}^{\mathrm{D}}(\xi,\xi)+(\xi+\xi^{-3})\lambda_\infty^{L-1}(1)-(\xi-\xi^{-1})^2\frac{d}{p}\lambda_\infty^{L-2}(1)+(1-\xi^{-2})^2[L+(\xi^2-1)i]\frac{d}{p}\lambda_\infty^{L-2}(1)$$
$$+(\xi-\xi^{-1})[\lambda_\infty^{L-i}(1)Z_{i-1}^{\mathrm{A}}(\xi,\xi)-\lambda_\infty^{i-1}(1)Z_{L-i}^{\mathrm{A}}(\xi,\xi)]+\Omega_L^{\mathrm{A}}(i;\xi,\xi)+\xi Z_{i-1}^{\mathrm{A}}(\xi,\xi)Z_{L-i}^{\mathrm{A}}(\xi,\xi). \tag{B19}$$

This completes our derivation of exact representations for $\Omega_L(i)$ in the four regions of the phase diagram characterized by different spectral properties of the truncated lattice propagator C_M.

[1] B. Derrida, M. R. Evans, V. Hakim, and V. Pasquier, J. Phys. A **26**, 1493 (1993).
[2] K. Krebs and S. Sandow, J. Phys. A **30**, 3165 (1997).
[3] F. H. L. Essler and V. Rittenberg, J. Phys. A **29**, 3375 (1996).
[4] N. Rajewski, A. Schadschneider, and M. Schreckenberg, J. Phys. A **29**, L305 (1996).
[5] N. Rajewski and M. Schreckenberg, Physica A **245**, 139 (1997).
[6] H. Hinrichsen, S. Sandow, and I. Peschel, J. Phys. A **29**, 2643 (1996).
[7] R. B. Stinchcombe and G. M. Schütz, Phys. Rev. Lett. **75**, 140 (1995).
[8] J. A. Zuk, Can. J. Phys. **70**, 257 (1992).
[9] N. Rajewsky, L. Santen, A. Schadschneider, and M. Schreckenberg, J. Stat. Phys. **92**, 151 (1998).
[10] D. Derrida, E. Domany, and D. Mukamel, J. Stat. Phys. **69**, 667 (1992).
[11] A. B. Kolomeisky, G. M. Schütz, E. B. Kolomeisky, and J. P. Straley, J. Phys. A **31**, 6911 (1998).